Dimension reduction of Karhunen-Loeve expansion for simulation of stochastic processes

Article *in* Journal of Sound and Vibration · November 2017

DOI: 10.1016/j.jsv.2017.07.016

3 authors:

Zhangjun Liu
China Three Gorges University

Zixin Liu
China Three Gorges University

Yongbo Peng
Tongji University

Journal of Sound and Vibration 408 (2017) 168–189

Contents lists available at ScienceDirect

Journal of Sound and Vibration

journal homepage: www.elsevier.com/locate/jsvi

Dimension reduction of Karhunen-Loeve expansion for simulation of stochastic processes

Zhangjun Liu [a], Zixin Liu [a], Yongbo Peng [b,*]

[a] Hubei Key Laboratory of Disaster Prevention and Reduction, China Three Gorges University, Yichang 443002, PR China

[b] State Key Laboratory of Disaster Reduction in Civil Engineering & Shanghai Institute of Disaster Prevention and Relief, Tongji University, Shanghai 200092, PR China

ARTICLE INFO

Article history:
Received 8 April 2017
Received in revised form
6 July 2017
Accepted 11 July 2017
Handling Editor: L.G. Tham

Keywords:
Karhunen-Loeve expansion
Dimension reduction
Random function
Stochastic process
Probability density evolution method
Nonlinear structures

ABSTRACT

Conventional Karhunen-Loeve expansions for simulation of stochastic processes often encounter the challenge of dealing with hundreds of random variables. For breaking through the barrier, a random function embedded Karhunen-Loeve expansion method is proposed in this paper. The updated scheme has a similar form to the conventional Karhunen-Loeve expansion, both involving a summation of a series of deterministic orthonormal basis and uncorrelated random variables. While the difference from the updated scheme lies in the dimension reduction of Karhunen-Loeve expansion through introducing random functions as a conditional constraint upon uncorrelated random variables. The random function is expressed as a single-elementary-random-variable orthogonal function in polynomial format (non-Gaussian variables) or trigonometric format (non-Gaussian and Gaussian variables). For illustrative purposes, the simulation of seismic ground motion is carried out using the updated scheme. Numerical investigations reveal that the Karhunen-Loeve expansion with random functions could gain desirable simulation results in case of a moderate sample number, except the Hermite polynomials and the Laguerre polynomials. It has the sound applicability and efficiency in simulation of stochastic processes. Besides, the updated scheme has the benefit of integrating with probability density evolution method, readily for the stochastic analysis of nonlinear structures.

1. Introduction

Engineering excitations such as earthquakes, wind and waves are of the stochastic processes in nature. Due to the essential non-stationarities of stochastic excitations and the significant nonlinearities of structural performance under these actions, the conventional spectrum-transfer schemes in frequency domain for structural stochastic analysis are not applicable. In this case, the power spectral density of stochastic excitations needs to be decomposed into sample processes in time domain for accurate stochastic response and reliability analysis of nonlinear structures.

Owing to the simple principles and ready-to-implement algorithm, random simulation method of stochastic processes receive great appeals in the past decades. Representative random simulation methods include (a) linear filter method [1], i.e., autoregressive (AR), moving average (MA) and autoregressive moving average (ARMA); (b) spectral representation

* Correspondence to: 1239 Siping Road, 803 Zonghe Building, Shanghai 200092, China.
E-mail addresses: liuzhangjun73@aliyun.com (Z. Liu), liuzixin1988@163.com (Z. Liu), pengyongbo@tongji.edu.cn (Y. Peng).

http://dx.doi.org/10.1016/j.jsv.2017.07.016
0022-460X/

method (SRM) [2]; (c) proper orthogonal decomposition (POD) [3], which is also referred to as the Karhunen-Loeve expansion [4]. In general, linear filter method has the ability of approximating the target spectral density matrix ultilizing a few parameters. While the implementation of algorithm is complicated, involving the estimation of categories, orders and parameters of models. It is thus limited in engineering applications in some cases. The spectral representation method has advantages of simple algorithm, rigorous theory and reliable simulation. This method, however, has to deal with a high-dimensional issue invovling a large number of random variables. In order to reduce the number of random variables, some efforts on the functional-set definition with respect to random variables from the first family of spectral representation [5] and on the random optimization with respect to frequencies and phase angles from the second family of spectral representation [6–8] were proceeded, respectively.

Power spectral density function is the critical component of spectral representation method, whereby the spectral representation method merely requires a fast Fourier transform (FFT) to implement the simulation of stochastic processes. While since the complete relationship between the spectral density function and the finite samples of stochastic processes is not fairly revealed, hundreds of terms need to be retained in order to accommodate the range of frequency and the uncertainty of phase angles, especially for the stochastic processes with short-time correlation. Consequently, it is appropriate to represent the randomness of stochastic processes by elementary variables so that the connection between random functions and sample processes could be readily established [9,10]. This thought is fully included in the Karhunen-Loeve expansion.

As a matter of fact, the Karhunen-Loeve expansion has a similar theoretical basis with the spectral representation method [5,11]. Both of them represent the stochastic processes as a summation of a series of deterministic functions modulated by a row of unrelated random coefficients (random variables). Compared with the spectral representation method, the Karhunen-Loeve expansion requires the solution of an eigenvalue problem [12]. It does not, of course, require the existence of a spectral density function, i.e., it is ready-made for non-stationary processes. However, the method is limited in practical application due to the difficulty of solving Fredholm integral equation. It still incurs, meanwhile, large number of random variables for the simulation of stochastic processes though the Karhunen-Loeve expansion has the optimality in the 2-norm sense. In order to solve the problem, some orthogonal expansion methods based on different orthonormal basis, e.g., generalized polynomial chaos [13], radial basis functions [14], and wavelet basis [15,16], were proposed. They are rigorously equivalent to the conventional Karhunen-Loeve expansion when the term number $N \to \infty$ [17,18]. In this manner, however, the number of random variables of orthogonal functions involved in a complete series expansion is still large.

An updated scheme of spectral representation was proposed through introducing the random functions as a conditional constraint [5]. This treatment bypasses the challenge of high-dimensional matter inherent in the conventional spectral representation. Moreover, the accuracy of simulation in the updated scheme can be improved through increasing the numbers of both expansion terms and representative samples. It was demonstrated that using the updated scheme with single-variable random functions, the accurate second-order statistics can be secured. Numerical investigations relevant to the simulation of stationary and non-stationary seismic acceleration processes demonstrated the applicability and efficiency of the method [5].

In this paper, a random function embedded Karhunen-Loeve expansion method for representation and simulation of stochastic processes is proposed. The updated scheme has a similar form to the conventional Karhunen-Loeve expansion, where the stochastic process is represented by a summation of a series of deterministic orthonormal basis and orthonormal random variables. A collection of random functions is introduced so as to implement the dimension reduction of discrete representation of stochastic processes. The remaining sections arranged in this paper are distributed as follows. Section 2 revisits the Karhunen-Loeve expansion for simulation of stochastic processes. The random function representation of kernel variables for Karhunen-Loeve expansion is detailed in Section 3, including a family of uncorrelated non-Gaussian variables and a family of uncorrelated Gaussian variables. Implementation procedure and error definition of the updated scheme are addressed in Section 4. For illustrative purposes, the simulation of random seismic ground motions is included in Section 5. Utilizing the probability density evolution method, case study on response analysis of randomly based-excited nonlinear structures is carried out in Section 6. The concluding remarks are included in Section 7.

2. Karhunen-Loeve expansion of stochastic processes

A physically based stochastic process $X(t)$ is a real-valued process, which is defined on the probability space $(\Omega, \mathcal{F}, P)$ and indexed on the bounded interval $[0, T]$. Without loss of generality, the stochastic process with a zero-mean and finite variance is investigated, where $E[X(t)] = 0$ and $E[X^2(t)]$ is bounded for all $t \in [0, T]$. The stochastic process can be approximately represented by a finite series of Karhunen-Loeve (K-L) expansion [19]

$$X(t) \doteq \sum_{i=1}^{N} \sqrt{\lambda_i}\xi_i f_i(t) \tag{1}$$

where $\{\xi_i\}_{i=1}^{N}$ denotes a set of uncorrelated standardized variables; N denotes the Karhunen-Loeve expansion terms; λ_i and

$f_i(t)$ are the eigenvalues and the eigenfunctions of covariance function $R(t_1, t_2)$, respectively. The covariance function $R(t_1, t_2)$ can be approximately decomposed as

$$R(t_1, t_2) = E[X(t_1)X(t_2)] \doteq \sum_{i=1}^{N}\sum_{j=1}^{N}\sqrt{\lambda_i\lambda_j}E[\xi_i\xi_j]f_i(t_1)f_j(t_2) = \sum_{i=1}^{N}\lambda_i f_i(t_1)f_i(t_2) \tag{2}$$

In essence, the eigenvalues λ_i and the eigenfunctions $f_i(t)$ are solutions of the second family of Fredholm integral equations:

$$\int_0^T R(t_1, t_2)f_i(t_1)\mathrm{d}t_1 = \lambda_i f_i(t_2) \tag{3}$$

The deterministic eigenfunctions $\left\{f_i(t)\right\}_{i=1}^{N}$ construct a set of orthonormal functions on the interval $[0, T]$, and satisfy the following orthogonality condition:

$$\int_0^T f_i(t)f_j(t)\mathrm{d}t = \delta_{ij} \tag{4}$$

where δ_{ij} is the Kronecker delta.

In Eq. (1), the mean-square relative error of the finite Karhunen-Loeve expansion series is defined as

$$\varepsilon_N = 1 - \frac{\sum_{i=1}^{N}\lambda_i}{\int_0^T R(t, t)\mathrm{d}t} \tag{5}$$

For a stationary stochastic process, the mean-square relative error ε_N can be written as

$$\varepsilon_N = 1 - \frac{\sum_{i=1}^{N}\lambda_i}{R(0)T} \tag{6}$$

It is noted that the collection of eigenvalues of the Eq. (3) is, at most, countable and strictly positive. Thus, the eigenvalues λ_i can be arranged in a decreasing order in Eq. (1). It has been proved that the truncated finite series in Eq. (1) are optimal, i.e., the mean-square relative error is minimized [20].

The primary task of Karhunen-Loeve expansion is thus to gain the eigenvalues and orthonormal eigenfunctions of the covariance function by solving the Fredholm integral Eq. (3). Unfortunately, the Fredholm integral is able to be solved analytically only in some rare cases. For practical engineering, the analytical solution of the Fredholm integral is unfeasible. One might have to refer to a numerical scheme. The numerical scheme commonly used in practices is detailed as follows.

(i) Select a set of orthonormal basis functions $\{\varphi_k(t)\}_{k=1}^{\infty}$, where the first M terms are used to evaluate the eigenvalues and eigenfunctions of the covariance function. In general, M must be equal to or larger than the terms number of Karhunen-Loeve expansion, i.e., $M \ge N$.

(ii) Calculate the covariance matrix $\mathbf{R}$

$$\mathbf{R} = \left[\rho_{ij}\right]_{M\times M} \tag{7}$$

where the component ρ_{ij} is defined as

$$\rho_{ij} = \int_0^T\int_0^T R(t_1, t_2)\varphi_i(t_1)\varphi_j(t_2)\mathrm{d}t_1\mathrm{d}t_2,\ i, j = 1, 2, \cdots, M \tag{8}$$

Obviously, the covariance matrix $\mathbf{R}$ is a real-valued symmetric matrix. The eigenvalues, therefore, of the real-valued symmetric matrix are real numbers and the associated eigenvectors are real vectors. Ordering the eigenvalues by decreasing values, moreover, all the eigenvalues are positive and goes to zero at infinity.

The eigenvalues $\tilde{\lambda}_i$ and the associated eigenvectors $\mathbf{\Phi}_i$ of the covariance matrix $\mathbf{R}$ can be obtained by solving the following eigenvalue problem

$$\mathbf{R}\mathbf{\Phi}_i = \tilde{\lambda}_i\mathbf{\Phi}_i \tag{9}$$

(iii) The eigenfunctions $f_i(t)$ in Eq. (3) can be approximated by a linear combination of the M-dimensional orthonormal basis functions:

$$f_i(t) \doteq \sum_{k=1}^{M}\phi_{ik}\varphi_k(t) \tag{10}$$

where ϕ_{ik} is the kth component of the eigenvector $\mathbf{\Phi}_i$, i.e., $\mathbf{\Phi}_i = \left\{\phi_{i1}, \phi_{i2}, \cdots, \phi_{ik}, \cdots, \phi_{iM}\right\}^{\mathrm{T}}$. In fact, $f_i(t)$ defined by Eq. (10) satisfies the orthogonality condition of Eq. (4), which is proved by

$$\begin{aligned}\int_0^T f_i(t)f_j(t)\mathrm{d}t &= \int_0^T \sum_{k=1}^{M} \phi_{ik}\varphi_k(t) \sum_{r=1}^{M} \phi_{jr}\varphi_r(t)\mathrm{d}t\\ &= \sum_{k=1}^{M}\sum_{r=1}^{M} \phi_{ik}\phi_{jr} \int_0^T \varphi_k(t)\varphi_r(t)\mathrm{d}t\\ &= \sum_{k=1}^{M}\sum_{r=1}^{M} \phi_{ik}\phi_{jr}\delta_{kr}\\ &= \sum_{k=1}^{M} \phi_{ik}\phi_{jk} = \mathbf{\Phi}_i^{\mathrm{T}}\mathbf{\Phi}_j = \delta_{ij}\end{aligned} \tag{11}$$

where the superscript T denotes transpose.

In the numerical scheme, a trigonometric orthonormal basis might be the alternative to the orthogonal set

$$\varphi_1(t) = \frac{1}{\sqrt{T}},\ \varphi_{2k}(t) = \frac{\sqrt{2}}{\sqrt{T}}\sin\left(\frac{2k\pi t}{T}\right),\ \varphi_{2k+1}(t) = \frac{\sqrt{2}}{\sqrt{T}}\cos\left(\frac{2k\pi t}{T}\right),\ k = 1, 2, \cdots \tag{12}$$

In addition, the eigenvalues λ_i of the Fredholm integral Eq. (3) can be approximated by the eigenvalues $\tilde{\lambda}_i$ of the covariance matrix $\mathbf{R}$ in Eq. (9), i.e., $\lambda_i \doteq \tilde{\lambda}_i$. In fact, substituting Eq. (10) into Eq. (3) and setting the error in Eq. (3) to be orthogonal to each basis function could derive the Eq. (9) [4]. When $M \to \infty$, the eigenvalues $\tilde{\lambda}_i$ of Eq. (9) and the eigenfunctions defined in Eq. (10) are completely equal to the eigenvalues λ_i and eigenfunctions of Eq. (3), respectively.

3. Random function representation of kernel variables

It is indicated in Karhunen-Loeve expansion that the uncorrelated standardized random variables ξ_i should satisfy the following conditions:

$$E[\xi_i] = 0,\ E[\xi_i\xi_j] = \delta_{ij} \tag{13}$$

where $E[\cdot]$ denotes the mathematical expectation.

Representation of wide-band stochastic processes such as seismic ground motions using the conventional Karhunen-Loeve expansion suffers from a computational challenge that hundreds of the uncorrelated random variables are often required, resulting in an unbearable Monte Carlo simulation (MCS) for stochastic dynamic analysis of engineering structures. This is a critical issue that the conventional spectral representation schemes are faced with as well. To overcome the issue, we implemented the efficient dimension reduction through transforming the hundreds of uncorrelated random variables into a random-function set with just one or two elementary random variables [5]. Similarly, the dimension reduction of Karhunen-Loeve expansion can be implemented using the constraint of random functions with a few of elementary random variables. In this paper, different types of random functions with just one elementary random variable are addressed in the following sections.

Suppose that the uncorrelated standardized random variables $\left\{\xi_i\right\}_{i=1}^{N}$ are orthogonal functions of the elementary random variable Θ, i.e., $\xi_i = g_i(\Theta)$, $i = 1, 2, \cdots, N$, Eq. (13) could be written as

$$E\ [\xi_i] = E\ [g_i(\Theta)] = \int_{-\infty}^{\infty} g_i(\theta)p_\Theta(\theta)\mathrm{d}\theta = 0,\ i = 1, 2, \cdots, N \tag{14a}$$

$$E\ [\xi_i\xi_j] = E\ [g_i(\Theta)g_j(\Theta)] = \int_{-\infty}^{\infty} g_i(\theta)g_j(\theta)p_\Theta(\theta)\mathrm{d}\theta = \delta_{ij},\ i, j = 1, 2, \cdots, N \tag{14b}$$

where $p_\Theta(\theta)$ denotes the probability density function of the elementary random variable Θ.

It is indicated that there would be of diversiform as to the random functions $\left\{g_i\right\}_{i=1}^{N}$ only if they satisfy the orthogonality conditions as mentioned in Eqs. (14a) and (14b). Table 1 presents the typical orthogonal functions and the probability density function (PDF) of elementary random variable.

3.1. Random functions for uncorrelated non-Gaussian variables

As seen from Table 1, there are 8 orthogonal functions representing uncorrelated standardized random variables with non-Gaussian distribution. The formulations of these functions are addressed as follows.

Table 1
Typical orthogonal functions and probability density function of elementary random variable.

Uncorrelated standardized random variables	Type of functions	Orthogonal functions	PDF of elementary random variable	Support of elementary random variable
Non-Gaussian	Polynomial format	Hermite polynomials	Gaussian	$(-\infty, \infty)$
		Laguerre polynomials	Exponential	$(0, \infty)$
		Legendre polynomials	Uniform	$(-1, 1)$
		1st Chebyshev polynomials	$\frac{1}{\pi\sqrt{1-\theta^2}}$	$(-1, 1)$
		2nd Chebyshev polynomials	$\frac{2}{\pi}\sqrt{1-\theta^2}$	$(-1, 1)$
	Trigonometric format	Trigonometric orthogonal basis	Uniform	$(0, 2\pi)$
		Sine function series (Hartley orthogonal basis)	Uniform	$(0, 2\pi)$
		Cosine function series	Uniform	$(0, \pi)$
Gaussian	Trigonometric format	Trigonometric orthogonal basis	Uniform	$(0, 2\pi)$
		Sine function series (Hartley orthogonal basis)	Uniform	$(0, 2\pi)$
		Cosine function series	Uniform	$(0, 2\pi)$

(i) For the Hermite orthogonal polynomial functions, the uncorrelated standardized random variables ξ_i can be defined as

$$\xi_i = g_i(\Theta) = \frac{1}{\sqrt{i!}} H_i(\Theta),\ i = 1, 2, \cdots, N \tag{15a}$$

where Θ denotes the elementary random variable on the interval $(-\infty, \infty)$, which is submitted to Gaussian distribution; $H_i(\cdot)$ is the Hermite polynomial function, and its recurrence formulas are given by

$$\begin{cases} H_{i+1}(x) = xH_i(x) - iH_{i-1}(x) \\ H_0(x) = 1,\ \ H_1(x) = x \end{cases} \tag{15b}$$

(ii) For the Laguerre orthogonal polynomial functions, the uncorrelated standardized random variables ξ_i can be defined as

$$\xi_i = g_i(\Theta) = L_i(\Theta),\ i = 1, 2, \cdots, N \tag{16a}$$

where Θ denotes the elementary random variable on the interval $(0, \infty)$, which is submitted to exponential distribution, and its probability density function $p_\Theta(\theta) = \exp(-\theta)$; $L_i(\cdot)$ is the Laguerre polynomial function, and its recurrence formulas are given by

$$\begin{cases} L_{i+1}(x) = \dfrac{2i+1-x}{i+1} L_i(x) - \dfrac{i}{i+1} L_{i-1}(x) \\ L_0(x) = 1,\ \ L_1(x) = 1 - x \end{cases} \tag{16b}$$

(iii) For Legendre orthogonal polynomial functions, the uncorrelated standardized random variables ξ_i can be defined as

$$\xi_i = g_i(\Theta) = \sqrt{2i+1}\, P_i(\Theta),\ i = 1, 2, \cdots, N \tag{17a}$$

where Θ denotes the elementary random variable on the interval $(-1, 1)$, which is submitted to uniform distribution; $P_i(\cdot)$ is the Legendre polynomial function, and its recurrence formulas are given by

$$\begin{cases} P_{i+1}(x) = \dfrac{2i+1}{i+1} xP_i(x) - \dfrac{i}{i+1} P_{i-1}(x) \\ P_0(x) = 1,\ \ P_1(x) = x \end{cases} \tag{17b}$$

(iv) For the first family of Chebyshev orthogonal polynomial functions, the uncorrelated standardized random variables ξ_i can be defined as

$$\xi_i = g_i(\Theta) = \sqrt{2}\, T_i(\Theta),\ i = 1, 2, \cdots, N \tag{18a}$$

where Θ denotes the elementary random variable on the interval $(-1, 1)$, which has the probability density function $p_\Theta(\theta) = \frac{1}{\pi\sqrt{1-\theta^2}}$; $T_i(\cdot)$ is the first family of Chebyshev polynomial function, and its recurrence formulas are given by

$$\begin{cases} T_{i+1}(x) = 2xT_i(x) - T_{i-1}(x) \\ T_0(x) = 1,\ \ T_1(x) = x \end{cases} \tag{18b}$$

Typically, the first family of Chebyshev orthogonal basis could be rewritten as [21]

$$\xi_i = g_i(\Theta) = \sqrt{2}\,T_i(\Theta) = \sqrt{2}\,\cos(i\,\arccos\Theta),\ i = 1, 2, \cdots, N \tag{18c}$$

(v) For the second family of Chebyshev orthogonal polynomial functions, the uncorrelated standardized random variables ξ_i can be defined as

$$\xi_i = g_i(\Theta) = U_i(\Theta),\ i = 1, 2, \cdots, N \tag{19a}$$

where Θ denotes the elementary random variable on the interval $(-1, 1)$, and its probability density function $p_\Theta(\theta) = \frac{2}{\pi}\sqrt{1-\theta^2}$; $U_i(\cdot)$ is the second family of Chebyshev polynomial function, and its recurrence formulas are given by

$$\begin{cases} U_{i+1}(x) = 2xU_i(x) - U_{i-1}(x) \\ U_0(x) = 1,\ \ U_1(x) = 2x \end{cases} \tag{19b}$$

Similarly, the second family of Chebyshev orthogonal basis could be rewritten as [21]

$$\xi_i = g_i(\Theta) = U_i(\Theta) = \frac{\sin[(i+1)\arccos\Theta]}{\sqrt{1-\Theta^2}},\ i = 1, 2, \cdots, N \tag{19c}$$

(vi) For trigonometric orthogonal basis, the uncorrelated standardized random variables ξ_i can be defined as

$$\xi_{2i-1} = g_{2i-1}(\Theta) = \sqrt{2}\,\sin(i\Theta + \alpha),\ \xi_{2i} = g_{2i}(\Theta) = \sqrt{2}\,\cos(i\Theta + \alpha);\ i = 1, 2, \cdots, \frac{N}{2} \tag{20}$$

where Θ denotes the uniformly distributed elementary random variable on the interval $(0, 2\pi)$; the parameter α is usually valued by $\pi/4$.

(vii) For sine function series, the uncorrelated standardized random variables ξ_i can be defined as

$$\xi_i = g_i(\Theta) = \sqrt{2}\,\sin(i\Theta + \alpha),\ i = 1, 2, \cdots, N \tag{21}$$

where Θ denotes the uniformly distributed elementary random variable on the interval $(0, 2\pi)$; the parameter α is usually valued by $\pi/4$.
Eq. (21) is also referred to as the Hartley orthogonal basis.

(viii) For cosine function series, the uncorrelated standardized random variables ξ_i can be defined as

$$\xi_i = g_i(\Theta) = \sqrt{2}\,\cos(i\Theta),\ i = 1, 2, \cdots, N \tag{22}$$

where Θ denotes the uniformly distributed elementary random variable on the interval $(0, \pi)$.

It is readily to demonstrate that the random variables $\{\xi_i\}_{i=1}^N$ defined by Eqs. (15)–(22) satisfy the conditions in Eqs. (14a) and (14b). In fact, although $\{\xi_i\}_{i=1}^N$ are a set of uncorrelated standardized random variables, they submit to a same probability distribution. As an example, it could be proved that the probability density functions of the random variables $\{\xi_i\}_{i=1}^N$ in Eq. (21) have a same non-Gaussian formulation. The proof is given as follows.

For function of a single elementary random variable, the probability distribution can be given as

$$p_{\xi_i}(\theta) = \sum_{k=1}^{m}\left|\frac{\mathrm{d}g_{i,k}^{-1}(\theta)}{\mathrm{d}\theta}\right| p_\Theta\left[g_{i,k}^{-1}(\theta)\right] = 2i \times \left|\frac{1}{i\sqrt{2-\theta^2}}\right| \times \frac{1}{2\pi} = \frac{1}{\pi\sqrt{2-\theta^2}},\ -\sqrt{2} < \theta < \sqrt{2} \tag{23}$$

where the function $g_{i,k}(\theta)$ is the kth monotonous segment of the function $g_i(\theta)$; $g_{i,k}^{-1}(\theta)$ is the inverse function of $g_{i,k}(\theta)$; m denotes the number of monotonous segments of $g_i(\theta)$.

Then, the cumulative distribution functions of the random variables ξ_i can be given by

$$F_{\xi_i}(\theta) = \begin{cases} 0 & \theta < -\sqrt{2} \\ \frac{1}{2} + \frac{1}{\pi}\arcsin\frac{\theta}{\sqrt{2}} & -\sqrt{2} \le \theta \le \sqrt{2} \quad \text{for } i = 1, 2, \cdots, N \\ 1 & \theta > \sqrt{2} \end{cases} \tag{24}$$

It is shown that the random variables $\{\xi_i\}_{i=1}^N$ in Eq. (21) are a set of uncorrelated non-Gaussian random variables with the same probability distribution. Similarly, the random variables $\{\xi_i\}_{i=1}^{N}$ in Eq. (20) or Eq. (22) also have a same cumulative distribution function; say Eq. (24). One might, moreover, prove that the random variables $\{\xi_i\}_{i=1}^{N}$ in Eq. (18) denoted by the first family of Chebyshev orthogonal basis have the same cumulative distribution function as Eq. (24).

3.2. Random functions for uncorrelated Gaussian variables

In order to gain a collection of uncorrelated standardized random variables $\{\bar{\xi}_i\}_{i=1}^{N}$ with the same Gaussian distribution, the inverse transform method of random variables can be used [22]:

$$\Phi(\bar{\xi}_i) = F_{\xi_i}(\xi_i),\ i = 1, 2, \cdots, N \tag{25}$$

where $\Phi(x)$ denotes the cumulative distribution function of Gaussian random variables, namely, $\Phi(x) = \frac{1}{\sqrt{2\pi}}\int_{-\infty}^{x}\exp\left(-\frac{t^2}{2}\right)\mathrm{d}t$. Using the inverse transform, Eq. (25) can be written as

$$\bar{\xi}_i = \Phi^{-1}\Big(F_{\xi_i}(\xi_i)\Big),\ i = 1, 2, \cdots, N \tag{26}$$

where $\Phi^{-1}(\cdot)$ denotes the inverse function of $\Phi(\cdot)$.

Then, successively substituting Eqs. (20)–(22) and Eq. (24) into Eq. (26), a set of uncorrelated standardized random variables $\{\bar{\xi}_i\}_{i=1}^{N}$ with the same Gaussian distribution can be obtained by

$$\bar{\xi}_{2i-1} = \Phi^{-1}\left[\frac{1}{2} + \frac{1}{\pi}\arcsin(\sin(i\Theta + \alpha))\right],\ \bar{\xi}_{2i} = \Phi^{-1}\left[\frac{1}{2} + \frac{1}{\pi}\arcsin(\cos(i\Theta + \alpha))\right],\ i = 1, 2, \cdots, \frac{N}{2} \tag{27}$$

where Θ denotes the uniformly distributed elementary random variable on the interval $(0, 2\pi)$; the parameter α is usually valued by $\pi/4$. Here, Eq. (27) is referred to as the Gaussian-trigonometric-orthogonal-basis, which could also be represented by

$$\bar{\xi}_i = \Phi^{-1}\left[\frac{1}{2} + \frac{1}{\pi}\arcsin(\sin(i\Theta + \alpha))\right],\ i = 1, 2, \cdots, N \tag{28}$$

where Θ denotes the uniformly distributed elementary random variable on the interval $(0, 2\pi)$; the parameter α is usually valued by $\pi/4$. Eq. (28) is referred to as the Gaussian-sine-function-series, i.e., Gaussian-Hartley-orthogonal-basis, which could also be represented by

$$\bar{\xi}_i = \Phi^{-1}\left[\frac{1}{2} + \frac{1}{\pi}\arcsin(\cos(i\Theta))\right],\ i = 1, 2, \cdots, N \tag{29a}$$

where Θ denotes the uniformly distributed elementary random variable on the interval $(0, \pi)$. Moreover, another kind of Gaussian-cosine-function-series can also be given by

$$\bar{\xi}_i = \Phi^{-1}\left[\frac{1}{2} + \frac{1}{\pi}\arcsin(\cos(i\Theta + \alpha))\right],\ i = 1, 2, \cdots, N \tag{29b}$$

where Θ denotes the uniformly distributed elementary random variable on the interval $(0, 2\pi)$; the parameter α is usually valued by $\pi/4$.

According to the equivalent relationship between the irrelevance and independence of Gaussian random variables, theoretically, $\{\bar{\xi}_i\}_{i=1}^{N}$ are also a set of independent random variables with Gaussian distributions.

4. Random function based Karhunen-Loeve expansion

4.1. Implement scheme

As mentioned in the previous section, the random functions with elementary random variable could serve as a random constraint for dimension reduction of Karhunen-Loeve expansion upon numerical simulation of stochastic processes. The steps of implement scheme are detailed as follows.

Step 1: Calculate the eigenvalues λ_i and eigenfunctions $f_i(t)$ of Karhunen-Loeve expansion using Eqs. (7)–(10). The number of Karhunen-Loeve expansion terms N is defined referring to the mean-square relative error ε_N.

Step 2: Determine the representative points' set. According to the support of the elementary random variable Θ, the representative points' set $\{\theta_j\}_{j=1}^{n_{\mathrm{sel}}}$ can be determined, where n_{sel} denotes the number of representative points.

Table 2
Discretion formulation of representative points' set of elementary random variable.

Orthogonal functions	Supports of elementary random variable	Discretion formulation and number of representative points $n_{\text{sel}} = 226, 422, 626, 818$
Hermite polynomials (non-Gaussian)	$(-\infty, \infty)$	$\theta_j = \frac{x_j - x_{j-1}}{2}$, $j = 2, 3, \cdots, (n_{\text{sel}} - 1)$, $\int_{-\infty}^{x_1} p_\Theta(\theta)\mathrm{d}\theta = \int_{x_{j-1}}^{x_j} p_\Theta(\theta)\mathrm{d}\theta = \int_{x_{n_{\text{sel}}-1}}^{\infty} p_\Theta(\theta)\mathrm{d}\theta = \frac{1}{n_{\text{sel}}}$
Laguerre polynomials (non-Gaussian)	$(0, \infty)$	$\theta_j = \frac{x_j - x_{j-1}}{2}$, $j = 2, 3, \cdots, (n_{\text{sel}} - 1)$, $\int_{0}^{x_1} p_\Theta(\theta)\mathrm{d}\theta = \int_{x_{j-1}}^{x_j} p_\Theta(\theta)\mathrm{d}\theta = \int_{x_{n_{\text{sel}}-1}}^{\infty} p_\Theta(\theta)\mathrm{d}\theta = \frac{1}{n_{\text{sel}}}$
Legendre polynomials (non-Gaussian)	$(-1, 1)$	$\theta_j = -1 + (j - 0.5) \times \frac{2}{n_{\text{sel}}}$, $j = 2, 3, \cdots, (n_{\text{sel}} - 1)$
1st Chebyshev polynomials (non-Gaussian)	$(-1, 1)$	$\theta_j = \frac{x_j - x_{j-1}}{2}$, $j = 2, 3, \cdots, (n_{\text{sel}} - 1)$, $\int_{-1}^{x_1} p_\Theta(\theta)\mathrm{d}\theta = \int_{x_{j-1}}^{x_j} p_\Theta(\theta)\mathrm{d}\theta = \int_{x_{n_{\text{sel}}-1}}^{1} p_\Theta(\theta)\mathrm{d}\theta = \frac{1}{n_{\text{sel}}}$
2nd Chebyshev polynomials (non-Gaussian)	$(-1, 1)$	$\theta_j = \frac{x_j - x_{j-1}}{2}$, $j = 2, 3, \cdots, (n_{\text{sel}} - 1)$, $\int_{-1}^{x_1} p_\Theta(\theta)\mathrm{d}\theta = \int_{x_{j-1}}^{x_j} p_\Theta(\theta)\mathrm{d}\theta = \int_{x_{n_{\text{sel}}-1}}^{1} p_\Theta(\theta)\mathrm{d}\theta = \frac{1}{n_{\text{sel}}}$
Trigonometric orthogonal basis (non-Gaussian)	$(0, 2\pi)$	$\theta_j = (j - 0.45) \times \frac{2\pi}{n_{\text{sel}}}$, $j = 2, 3, \cdots, (n_{\text{sel}} - 1)$
Hartley orthogonal basis (non-Gaussian)	$(0, 2\pi)$	$\theta_j = (j - 0.45) \times \frac{2\pi}{n_{\text{sel}}}$, $j = 2, 3, \cdots, (n_{\text{sel}} - 1)$
Cosine function series (non-Gaussian)	$(0, \pi)$	$\theta_j = (j - 0.45) \times \frac{\pi}{n_{\text{sel}}}$, $j = 2, 3, \cdots, (n_{\text{sel}} - 1)$
Trigonometric orthogonal basis (Gaussian)	$(0, 2\pi)$	$\theta_j = (j - 0.6) \times \frac{2\pi}{n_{\text{sel}}}$, $j = 2, 3, \cdots, (n_{\text{sel}} - 1)$
Hartley orthogonal basis (Gaussian)	$(0, 2\pi)$	$\theta_j = (j - 0.6) \times \frac{2\pi}{n_{\text{sel}}}$, $j = 2, 3, \cdots, (n_{\text{sel}} - 1)$
Cosine function series (Gaussian)	$(0, 2\pi)$	$\theta_j = (j - 0.6) \times \frac{2\pi}{n_{\text{sel}}}$, $j = 2, 3, \cdots, (n_{\text{sel}} - 1)$

Meanwhile, the assigned probabilities of representative points $\{P_j\}_{j=1}^{n_{\text{sel}}}$ are readily to be calculated, which satisfies the condition $\sum_{j=1}^{n_{\text{sel}}} P_j = 1$. The discretion formulation of representative points' set of elementary random variable are showed in Table 2.

The equal-probability-assignment scheme for point-set discretion is used. In this scheme, the assigned probability of each representative point is the same. It is equivalent to the uniformly-spaced formulation for the random variables submitting to uniform distribution. While there is a big difference between the equal-probability-assignment scheme and the uniformly-spaced scheme for the non-uniform random variables. In the former, the first representative point is defined as the right endpoint of the first subdivision domain no matter that the distribution domain of random variables is bounded or unbounded, and the last representative point is defined as the left endpoint of the last subdivision domain. The most remaining representative points are defined according to the formulations shown in Table 2.

Step 3: Generate the time histories of representative samples. Substituting representative point θ_j into the random functions, e.g., Eqs. (15)–(22) or Eqs. (27)–(29), a set of deterministic values of uncorrelated standardized random variables $\{\xi_i\}_{i=1}^{N}$ could be derived. The ith representative sample of stochastic process can be then generated by Karhunen-Loeve expansion; say Eq. (1), of which the assigned probability is denoted by $1/n_{\text{sel}}$. A set of representative samples of stochastic process is thus obtained in case that all the n_{sel} representative samples are orderly simulated.

4.2. Error definition

In order to quantitatively assess the difference between the target process and the simulated process, three families of average relative errors are defined as follows.

The average relative error upon the mean of stochastic process is defined as

$$\varepsilon_{\text{m},1} = \frac{1}{N_t}\sum_{k=1}^{N_t}\left|\frac{\mu(t_k) - \hat{\mu}(t_k)}{\mu(t_k)}\right|, \text{ for } \mu(t) = E[X(t)] \neq 0 \tag{30a}$$

or

$$\varepsilon_{\mathrm{m},1} = \frac{1}{N_t}\sum_{k=1}^{N_t}\left|\frac{\mu(t_k) - \hat{\mu}(t_k)}{\sigma(t_k)}\right|, \ \text{for } \mu(t) = E[X(t)] = 0 \tag{30b}$$

The average relative error upon the standard deviation function of stochastic process is defined as

$$\varepsilon_{\mathrm{m},2} = \frac{1}{N_t}\sum_{k=1}^{N_t}\left|\frac{\sigma(t_k) - \hat{\sigma}(t_k)}{\sigma(t_k)}\right| \tag{31}$$

where $\mu(t_k)$ and $\sigma(t_k)$ denote the values of mean and standard deviation of the target process at the kth time instant, respectively; $\hat{\mu}(t_k)$ and $\hat{\sigma}(t_k)$ denote the values of mean and standard deviation of the simulated process at the kth time instant, respectively; N_t represents the number of time instants involved in representative samples, i.e., $N_t = T/\Delta t$, where Δt denotes the time step of representative samples.

The average relative error upon the power spectral density function for stationary processes is defined as

$$\varepsilon_{\mathrm{m},3} = \frac{1}{N_f}\sum_{k=1}^{N_f}\left|\frac{S(\omega_k) - \hat{S}(\omega_k)}{S(\omega_k)}\right| \tag{32}$$

where $S(\omega_k)$ represents the value of the target power spectrum at the kth frequency point; $\hat{S}(\omega_k)$ represents the value of the simulated power spectrum at the kth frequency point. N_f represents the number of frequency points involved in power spectral density, i.e., $N_f = \omega_u/\Delta\omega$, where ω_u denotes the upper cut-off frequency, and $\Delta\omega$ denotes the frequency interval.

The above definitions of average relative errors rely mainly upon the number of representative samples of stochastic

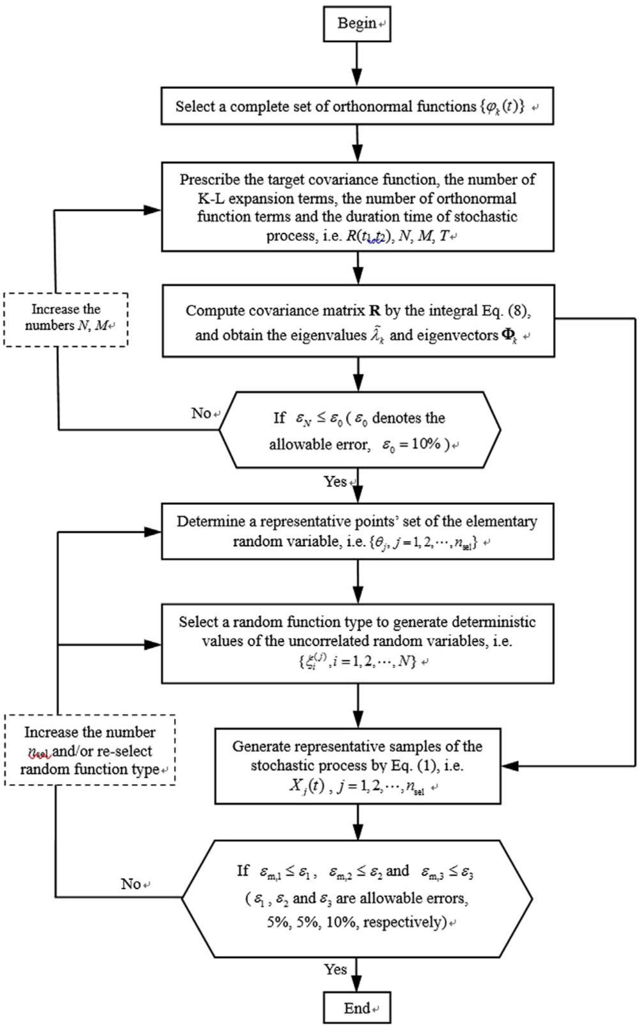

Fig. 1. Flow chart of the proposed scheme to simulate stochastic processes.

process, i.e., the number of representative points n_{sel} of the elementary random variable, which is determined in case that the fitting error of second-order statistics between the target process and the simulated process is accepted. Flow chart of random function based Karhunen-Loeve expansion is shown in Fig. 1. Some remarks on the random function based Karhunen-Loeve expansion, i.e., an updated Karhunen-Loeve expansion, are drawn as follows:

Remark 1. In the conventional Karhunen-Loeve expansion, say Eq. (1), the number of random variables, herein labeled as randomness degree, of the stochastic process is defined as *N*. While in the updated Karhunen-Loeve expansion, the number of random variables could be defined as 1. It is shown that the randomness degree of stochastic processes can be effectively reduced by applying the constraint of random functions. It is just similar to the Rayleigh-Ritz method in dynamics of structures, transforming the multi-degree-of-freedom system into the single-degree-of-freedom system by introducing shape functions or basis vectors. The basic conditions shown in Eq. (13) or Eq. (14) are analog to the displacement boundary conditions in the Rayleigh-Ritz method, while the random functions are analog to the displacement shape functions.

Remark 2. Only one elementary random variable is needed in the updated Karhunen-Loeve expansion to represent the stationary and non-stationary stochastic processes for practical applications. This treatment provides a ready integration with the probability density evolution method, prompting the accurate response analysis and dynamic reliability of randomly-excited nonlinear structural systems.

Remark 3. The uncorrelated random variables $\{\xi_i\}_{i=1}^N$ in the updated Karhunen-Loeve expansion are generated directly by random functions; say Eqs. (15)–(22) or Eqs. (27)–(29). However, in the random function based spectral representation [5], the uncorrelated random variables $\{\xi_i\}_{i=1}^N$ generally need one-to-one mapping transform from the defined random functions. It is just the technical benefit of the Karhunen-Loeve expansion of which the series of terms in Karhunen-Loeve expansion are arranged in a descending order of eigenvalues, consistent with the order of the uncorrelated random variables defined by random functions. While the series of terms in spectral representation are arranged according to the frequency components of power spectral density or evolutionary spectrum.

Remark 4. The total number of terms involved in the updated Karhunen-Loeve expansion is the same as the conventional one. They both remain the terms associated with the most energy of the stochastic process. The finite Karhunen-Loeve expansion series satisfies with an acceptable mean-square relative error defined in Eqs. (5) and (6). Although possessing a same number of truncated terms, the updated Karhunen-Loeve expansion gains a better simulation efficiency with higher accuracy and fewer samples through a dimension reduction technique in conjunction with random functions.

5. Simulation of stochastic seismic ground motions

5.1. Stationary seismic acceleration process

In earthquake engineering community, the seismic ground motion is usually assumed to be a real-valued stochastic process with zero-mean, and its power spectral density function serves as the key statistics for the representation of stationary stochastic processes. In this paper, the Clough-Penzien (C-P) power spectrum is used to simulate the stochastic ground motion acceleration process $X_g(t)$, of which a two-sided spectral density is given by [23]

$$S(\omega) = S_0 \frac{\omega_g^4 + 4\zeta_g^2\omega_g^2\omega^2}{(\omega^2 - \omega_g^2)^2 + 4\zeta_g^2\omega_g^2\omega^2} \frac{\omega^4}{(\omega^2 - \omega_f^2)^2 + 4\zeta_f^2\omega_f^2\omega^2} \tag{33}$$

where S_0 denotes the intensity factor of power spectrum; ω_g and ζ_g are the filter parameters of the well-known Kanai-Tajimi power spectrum representing the dominant frequency and critical damping of the soil layer, respectively. ω_f and ζ_f are parameters of a second filter which is introduced to secure a finite power for the ground displacement. These filter parameters were valued and addressed by Der Kiureghian and Neuenhofer [24], Seya et al. [25] and Deodatis [26]. In this paper, as a case of deep cohesionless soils, the parameters are valued by $\omega_g = 5\pi$ rad/s, $\zeta_g = 0.6$, $\omega_f = 0.5\pi$ rad/s, $\zeta_f = 0.6$.

The intensity factor of power spectrum S_0 has the functional relationship with the peak ground acceleration (PGA) as follows [25]

$$S_0 = \frac{A_p^2}{\gamma^2\pi\omega_g\left(2\zeta_g + \frac{1}{2\zeta_g}\right)} \tag{34}$$

where A_p denotes the PGA value; γ denotes the peak factor and is valued by 3.0 for deep cohesionless soils.

According to the Wiener-Khintchine theorem, the auto-correlation function of the ground motion acceleration process, as an inverse Fourier transform of Eq. (33), is given by

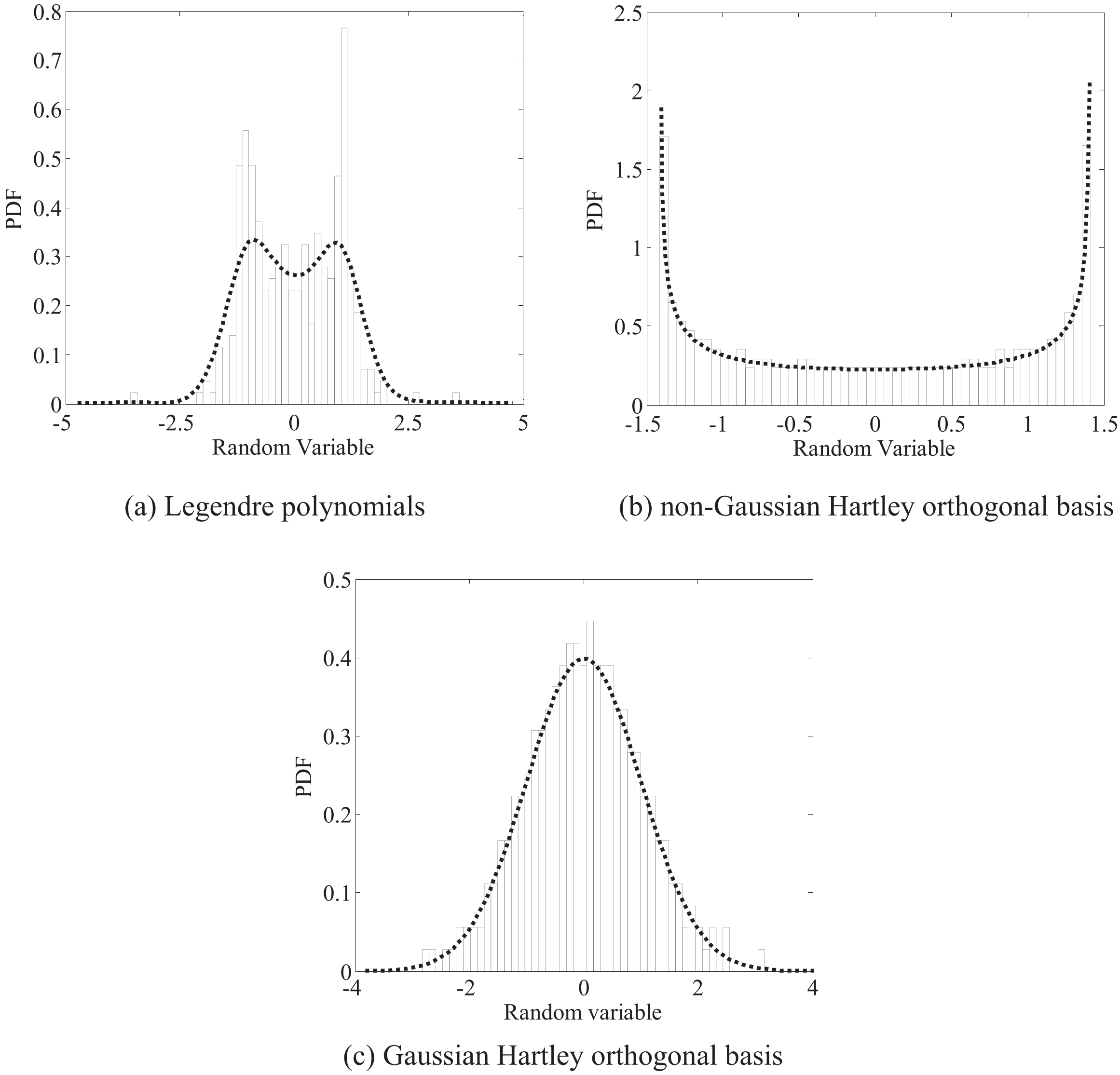

Fig. 2. Scaled histograms and probability density functions of random variable ξ_{200} represented by: (a) Legendre polynomials; (b) non-Gaussian Hartley orthogonal basis; and (c) Gaussian Hartley orthogonal basis.

$$R(t_1, t_2) = R(t_2 - t_1) = R(\tau) = \int_{-\infty}^{\infty} S(\omega) e^{\mathrm{i}\omega\tau} \mathrm{d}\omega = \mathrm{i}2\pi S_0 \sum_{j=1}^{4} R_j(\tau) \tag{35}$$

where i denotes the imaginary unit, i.e., $\mathrm{i} = \sqrt{-1}$; the formulations of $R_j(\tau)$ are given by

$$R_1(\tau) = \frac{\omega_g^4 + 4\zeta_g^2\omega_g^2\omega_1^2}{(\omega_1 - \omega_2)(\omega_1 - \omega_3)(\omega_1 - \omega_4)} \frac{\omega_1^4 \exp(\mathrm{i}|\tau|\omega_1)}{(\omega_1^2 - \omega_f^2)^2 + 4\zeta_f^2\omega_f^2\omega_1^2} \tag{36a}$$

$$R_2(\tau) = \frac{\omega_g^4 + 4\zeta_g^2\omega_g^2\omega_2^2}{(\omega_2 - \omega_1)(\omega_2 - \omega_3)(\omega_2 - \omega_4)} \frac{\omega_2^4 \exp(\mathrm{i}|\tau|\omega_2)}{(\omega_2^2 - \omega_f^2)^2 + 4\zeta_f^2\omega_f^2\omega_2^2} \tag{36b}$$

$$R_3(\tau) = \frac{\omega_g^4 + 4\zeta_g^2\omega_g^2\omega_5^2}{(\omega_5^2 - \omega_g^2)^2 + 4\zeta_g^2\omega_g^2\omega_5^2} \frac{\omega_5^4 \exp(\mathrm{i}|\tau|\omega_5)}{(\omega_5 - \omega_6)(\omega_5 - \omega_7)(\omega_5 - \omega_8)} \tag{36c}$$

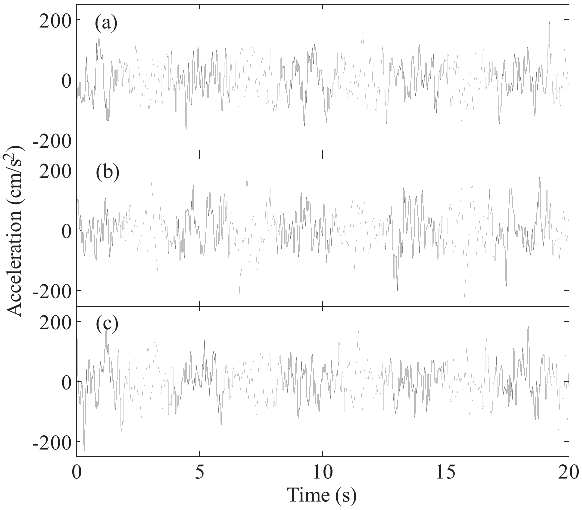

Fig. 3. Representative time histories simulated by the proposed scheme with random functions: (a) Legendre polynomials; (b) non-Gaussian Hartley orthogonal basis; and (c) Gaussian Hartley orthogonal basis in case of sample number $n_{\rm sel} = 626$.

$$R_4(\tau) = \frac{\omega_g^4 + 4\zeta_g^2\omega_g^2\omega_6^2}{(\omega_6^2 - \omega_g^2)^2 + 4\zeta_g^2\omega_g^2\omega_6^2}\frac{\omega_6^4\exp(\mathrm{i}|\tau|\omega_6)}{(\omega_6 - \omega_5)(\omega_6 - \omega_7)(\omega_6 - \omega_8)} \tag{36d}$$

where

$$\omega_1 = \sqrt{1 - \zeta_g^2}\,\omega_g + \mathrm{i}\zeta_g\omega_g,\ \omega_2 = -\sqrt{1 - \zeta_g^2}\,\omega_g + \mathrm{i}\zeta_g\omega_g,\ \omega_3 = \omega_1^*,\ \omega_4 = \omega_2^*,$$

$$\omega_5 = \sqrt{1 - \zeta_f^2}\,\omega_f + \mathrm{i}\zeta_f\omega_f,\ \omega_6 = -\sqrt{1 - \zeta_f^2}\,\omega_f + \mathrm{i}\zeta_f\omega_f,\ \omega_7 = \omega_5^*,\ \omega_8 = \omega_6^*.$$

where the symbol "*" denotes conjugate complex.

For the cases of simulation of the stationary and the non-stationary seismic acceleration processes, the number of Karhunen-Loeve expansion terms is defined as $N = 600$, and the number of involved eigenfunctions $M = 600$; the duration time of ground motion is defined as $T = 20$ s; the time interval of representative samples $\Delta t = 0.01$ s; and the PGA $A_p = 0.2g = 196$ cm/s^2 where g denotes the value of gravitational acceleration.

Fig. 2 shows the scaled histograms of the random variable ξ_{200} represented by the Legendre polynomials, the non-Gaussian Hartley orthogonal basis and the Gaussian Hartley orthogonal basis, respectively, using the statistical method. Their analytical probability density functions are exposed as well. It is seen that the uncorrelated random variables represented by the Legendre polynomials and the non-Gaussian Hartley orthogonal basis feature an obvious non-Gaussian distribution; while the uncorrelated random variables represented by the Gaussian Hartley orthogonal basis feature a Gaussian distribution.

Accordingly, the time histories of seismic acceleration processes could be simulated using the random function based Karhunen-Loeve expansion. Fig. 3 shows the representative samples simulated by the proposed scheme with random functions: the Legendre polynomials, the non-Gaussian Hartley orthogonal basis, and the Gaussian Hartley orthogonal basis, in case of representative points number $n_{\rm sel} = 626$. It is seen that the stationary characteristics are well exposed in the simulated processes. Comparison between the target statistics and those of simulated stationary seismic acceleration processes with respect to the mean, standard deviation and power spectral density are shown in Fig. 4. One might readily realize that the updated Karhunen-Loeve expansion with random functions in the Legendre polynomials, the non-Gaussian Hartley orthogonal basis, and the Gaussian Hartley orthogonal basis has the capacity of gaining desirable simulation results, respectively. Fig. 5 shows the scaled histograms and probability density functions of simulated stationary seismic acceleration processes at the typical instant of time $t = 10$ s using the statistical method and the Gaussian estimation, respectively. It is clear that the simulated processes has a serious Gaussianity owing to the central limit theorem though the variables in the random functions of the updated scheme might be non-Gaussian. The simulation results by the conventional Karhunen-Loeve expansion with the representative points number $n_{\rm sel} = 626$ is exposed as well; see Fig. 5(d), where the MCS is employed to gain the representative samples associated with hundreds of random variables. It is seen that the updated and conventional Karhunen-Loeve expansion have a consistent result, but the former operates efficiently through a dimension-reduction technique. In order to convince the results by the statistical method, the probability density evolution method is employed herein to derive the exact PDFs. It is indeed proved that the histograms have a sufficient accuracy since they match well with the curves derived from the probability density evolution method.

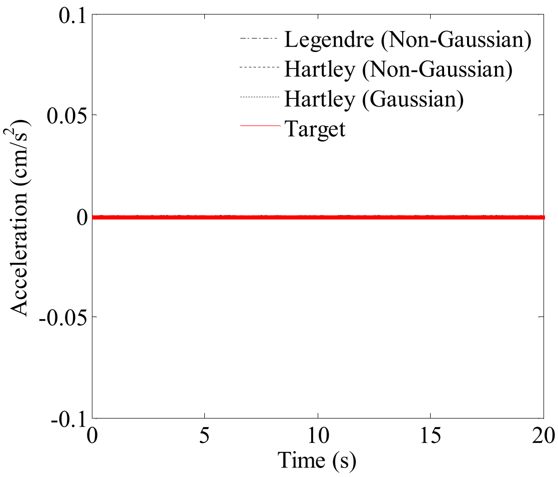

(a) mean

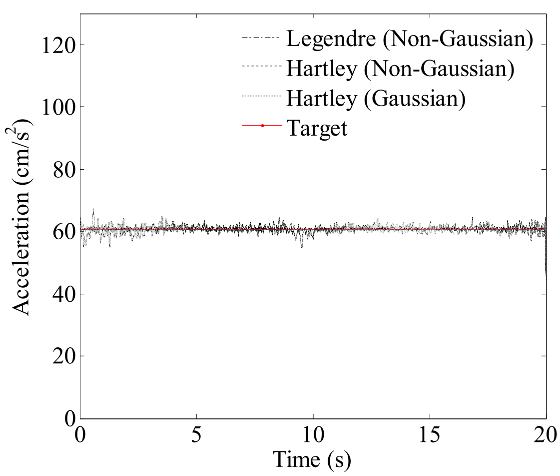

(b) standard deviation

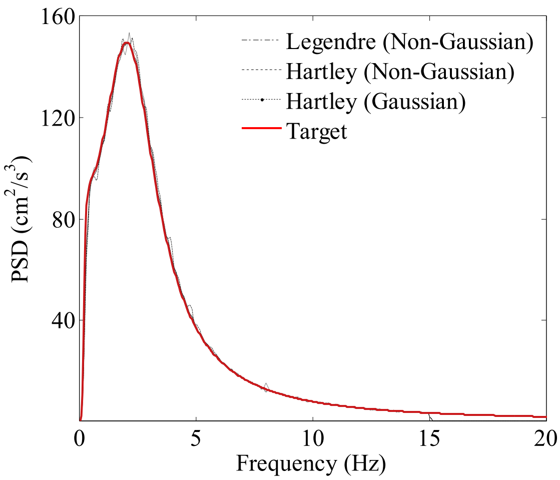

(c) power spectral density

Fig. 4. Comparison between target statistics and those of simulated stationary seismic acceleration processes with respect to: (a) mean; (b) standard deviation; and (c) power spectral density in case of sample number $n_{sel} = 626$.

We further evaluate the numerical accuracy of the random function based Karhunen-Loeve expansion with respect to the number of representative points. For this purpose, the numbers of representative time histories $n_{sel} = 226$, 422, 626 and 818, derived from probability-space partition, are involved. Due to the unbounded supports of the elementary random variables, the Hermite polynomials and the Laguerre polynomials are not suitable for the logical simulation of a physical process such as seismic ground motions. In this study, the remaining 9 random functions are investigated. It is seen from Fig. 6 that the average relative errors using the introduced random functions against the target process, upon the mean, standard deviation and power spectral density, are all reduced as the number of representative time histories increases. The average relative errors decrease quickly in case of a small number; while they decrease slowly in case that the number is around 600. In case of a moderate sample number; say $n_{sel} = 626$, the random functions gain a satisfied result, corresponding to 5% less average relative errors upon mean and standard deviation and 10% less average relative error upon power spectral density.

It is also indicated in Fig. 6 that the random functions accommodate a serious zero-mean stochastic process where the amplitude of average relative errors are around 10^{-8}. For the orthogonal polynomials, it is recommended to preferentially use the Legendre polynomials and the 1st Chebyshev polynomials. While for the three types of trigonometric functions, all of them can be selected to be used since their relative errors are very close no matter the generated uncorrelated random variables are non-Gaussian or Gaussian distribution. For convenience of illustration, the Legendre polynomials, the non-Gaussian Hartley orthogonal basis and the Gaussian Hartley orthogonal basis are investigated as simulation examples in this paper.

In order to further illustrate the advantage of the updated Karhunen-Loeve expansion, the accuracy of the conventional

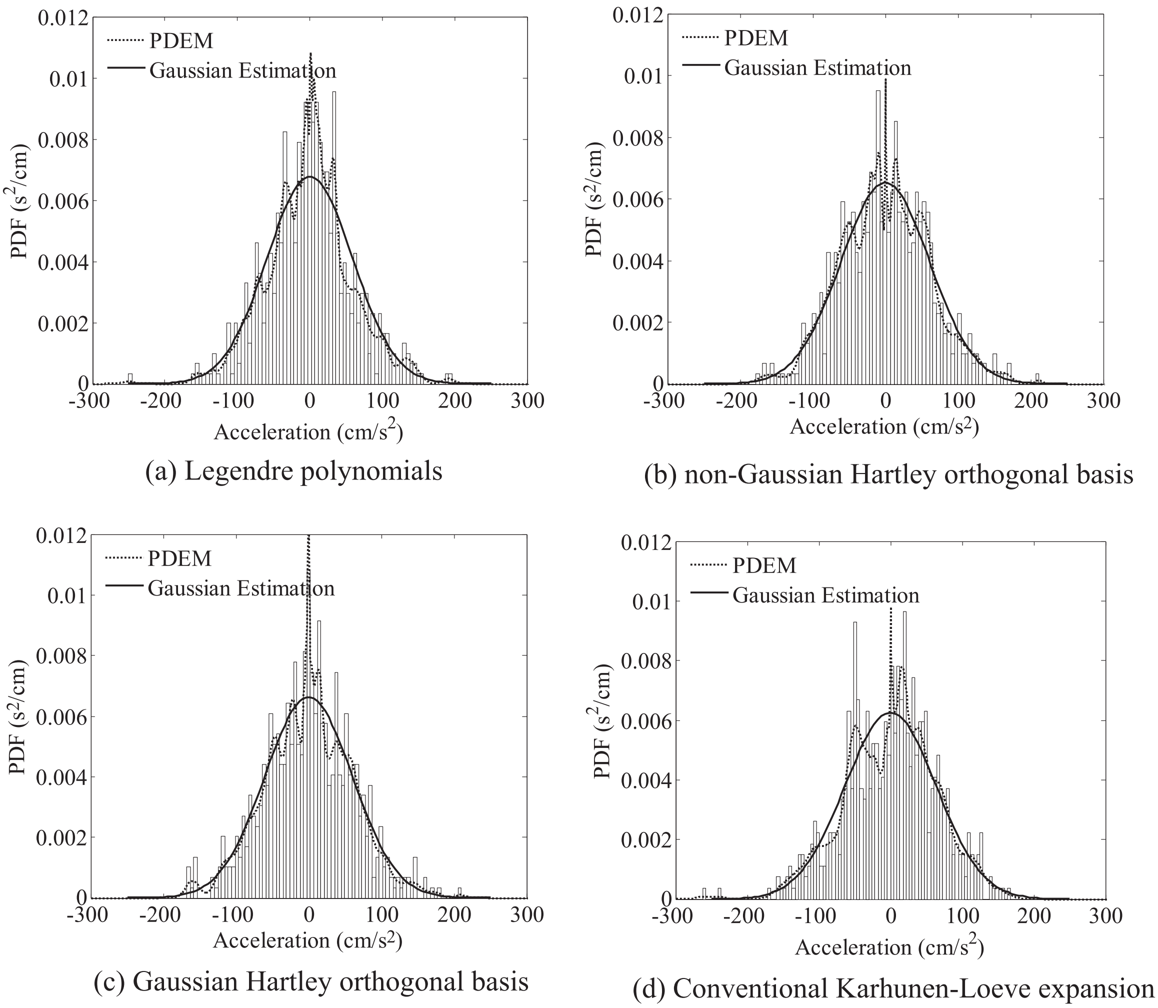

Fig. 5. Scaled histograms and probability density functions of simulated stationary seismic acceleration processes at the typical instant of time $t = 10$ s using the updated and conventional schemes: (a) Legendre polynomials; (b) non-Gaussian Hartley orthogonal basis; (c) Gaussian Hartley orthogonal basis; and (d) conventional Karhunen-Loeve expansion.

Karhunen-Loeve expansion is investigated in case of the sample number $n_{sel} = 626$. It is seen from Table 3 that the updated scheme gains an extremely smaller error upon mean and substantially smaller error upon standard deviation and power spectral density than the conventional scheme, except the error upon the power spectral density using the Legendre polynomial. Therefore, the updated scheme has a better simulation result than the conventional scheme, which is, moreover, readily to be combined with the probability density evolution method (PDEM) in proceeding the dynamic responses and reliability assessment of engineering structures.

Besides, the kernel variables represented by the random functions should satisfy the basic conditions associated with the zero mean, unit standard deviation and orthogonality, as shown in Eq. (14). In numerical simulation, the kernel variables are usually standardized so as to meet with these requirements.

5.2. Non-stationary seismic acceleration process

Generally, the non-stationary seismic ground motion could be gained through a modulation technique on the stationary seismic ground motion. The modulation techniques typically involve uniform and non-uniform modulations. The uniformly modulated non-stationary seismic acceleration process is widely used and can be expressed as the product of deterministic modulation function and stationary acceleration process:

$$\tilde{X}_g(t) = A(t)X_g(t) \tag{37}$$

where $\tilde{X}_g(t)$ denotes non-stationary seismic acceleration process with zero-mean; $X_g(t)$ denotes stationary seismic

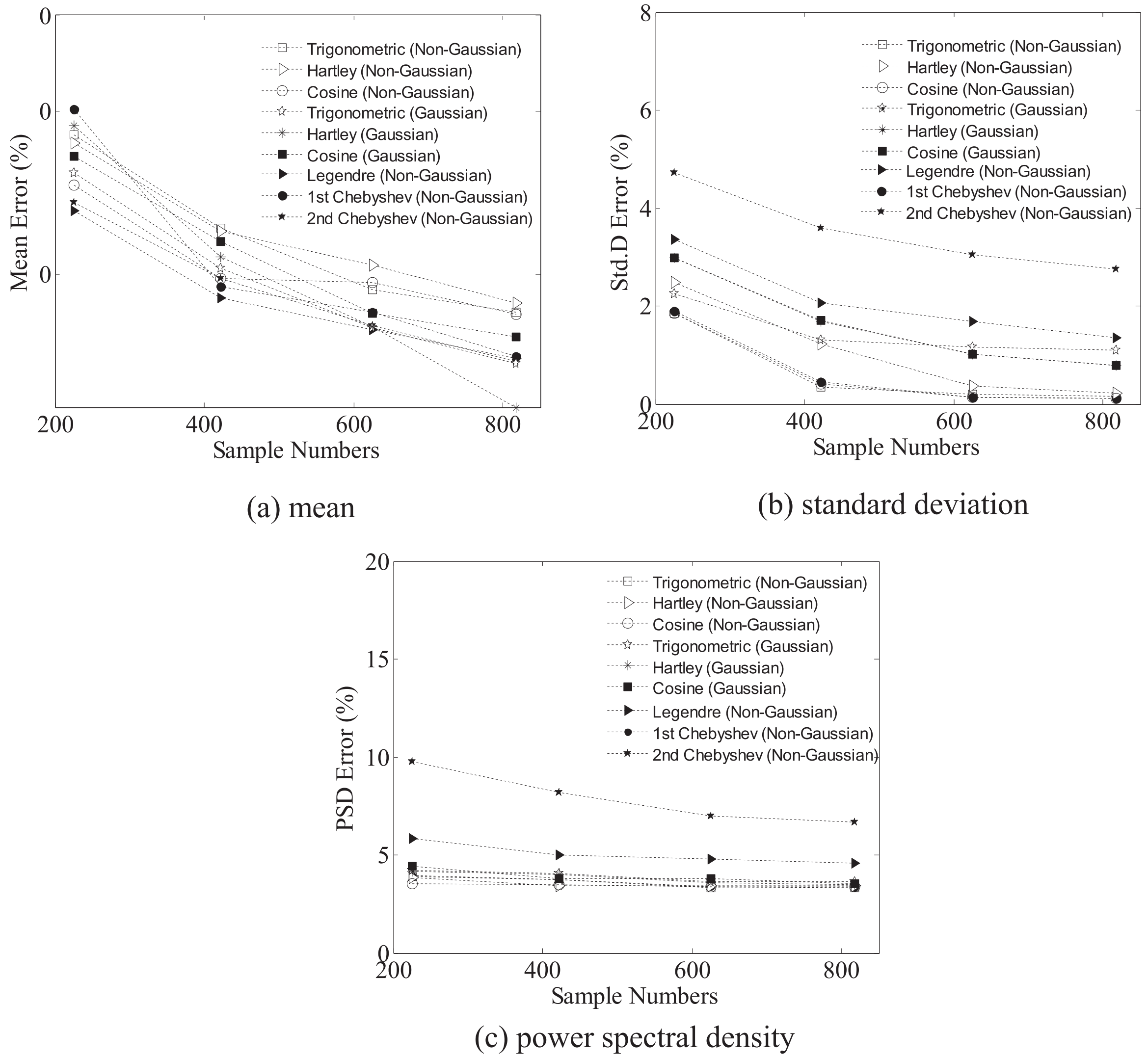

Fig. 6. Average relative errors of the simulated stationary processes upon: (a) mean; (b) standard deviation; and (c) power spectral density using random function based scheme with different sample numbers.

Table 3
Comparisons of average relative errors of stationary stochastic processes simulated by the updated and conventional Karhunen-Loeve expansions.

Representation schemes ($n_{sel} = 626$)		Average relative errors		
		Mean	Standard deviation	Power spectral density
Conventional Karhunen-Loeve expansion		3.22%	2.30%	4.70%
Updated Karhunen-Loeve expansion	Legendre (Non-Gaussian)	7.91×10^{-10}	1.68%	4.79%
	Hartley (Non-Gaussian)	1.04×10^{-9}	0.36%	3.45%
	Hartley (Gaussian)	8.02×10^{-10}	1.02%	3.58%

acceleration process with zero-mean; $A(t)$ denotes the deterministic modulation function reflecting intensity-related non-stationary characteristics of seismic acceleration in time domain, which can be expressed as follow [27]:

$$A(t) = \left[\frac{t}{c}\exp\left(1 - \frac{t}{c}\right)\right]^d \tag{38}$$

where c denotes average arrival time of peak ground acceleration; the parameter d is used to control the shape of $A(t)$. In this paper, $c = 4$ s and $d = 1$.

Table 4
Comparisons of average relative errors of non-stationary stochastic processes simulated by the updated and conventional Karhunen-Loeve expansions.

Representation schemes (n_{sel} = 626)		Average relative errors		
		Mean	Standard deviation	Power spectral density at 7.5 s
Conventional Karhunen-Loeve expansion		3.24%	2.45%	8.26%
Updated Karhunen-Loeve expansion	Legendre (Non-Gaussian)	7.81×10^{-10}	2.36%	9.07%
	Hartley (Non-Gaussian)	1.09×10^{-9}	0.57%	6.49%
	Hartley (Gaussian)	8.02×10^{-10}	1.26%	6.75%

The auto-correlation function of non-stationary seismic acceleration process can thus be expressed as

$$\tilde{R}(t_1, t_2) = A(t_1)A(t_2)R(t_2 - t_1) \tag{39}$$

where $R(t_2 - t_1) = R(\tau)$ denotes the auto-correlation function of stationary seismic acceleration process, which is shown in Eq. (35). Meanwhile, the evolutionary power spectral density function of non-stationary seismic acceleration process $\tilde{X}_g(t)$ is expressed as

$$\tilde{S}(t, \omega) = A^2(t)S(\omega) \tag{40}$$

According to statistical relationship of stochastic processes, the mean and variance of non-stationary seismic acceleration process are derived as follows, respectively:

$$E\left[\tilde{X}_g(t)\right] = A(t)E\left[X_g(t)\right] = 0 \tag{41}$$

$$\sigma^2_{\tilde{X}_g} = E\left[\tilde{X}_g^2(t)\right] = \tilde{R}(t, t) = \int_{-\infty}^{\infty} \tilde{S}(t, \omega)\mathrm{d}\omega = A^2(t) \int_{-\infty}^{\infty} S(\omega)\mathrm{d}\omega \tag{42}$$

Fig. 7 shows the representative samples of non-stationary seismic acceleration processes simulated by the updated Karhunen-Loeve expansion with the Legendre polynomials, the non-Gaussian Hartley orthogonal basis and the Gaussian Hartley orthogonal basis, respectively, in case of the sample number n_{sel} = 626. It is seen that there arise obvious non-stationary characteristics in the simulated processes. One might realize that the variations between sample processes using the updated Karhunen-Loeve expansion with the three random functions seem significant, where the time lengths of large-amplitude segments are different evidently. In fact, the sample processes using the same random function arise the remarkable discrepancy as well. While there is merely consistent in the statistical processes using the three random functions.

Comparison between the target statistics and those of simulated non-stationary seismic acceleration processes with respect to the mean and standard deviation are shown in Fig. 8. It is indicated that similar to the stationary cases, the updated Karhunen-Loeve expansion with the random functions in the Legendre polynomials, the non-Gaussian Hartley orthogonal basis, and the Gaussian Hartley orthogonal basis gain desirable simulation results. Fig. 9 shows the target power

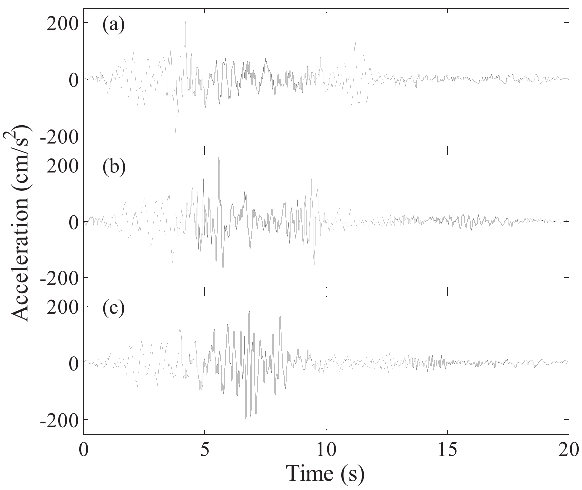

Fig. 7. Representative time histories of non-stationary seismic acceleration processes simulated by updated schemes with random functions: (a) Legendre polynomials; (b) non-Gaussian Hartley orthogonal basis; and (c) Gaussian Hartley orthogonal basis in case of sample numbern_{sel} = 626.

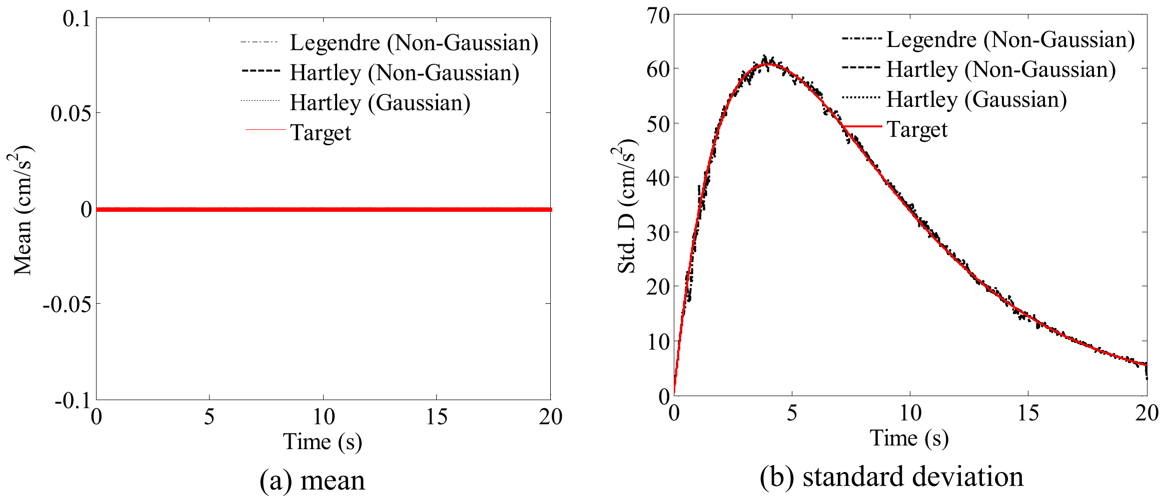

Fig. 8. Comparison between target statistics and those of simulated non-stationary seismic acceleration processes as to: (a) mean, and (b) standard deviation in case of sample number $n_{sel} = 626$.

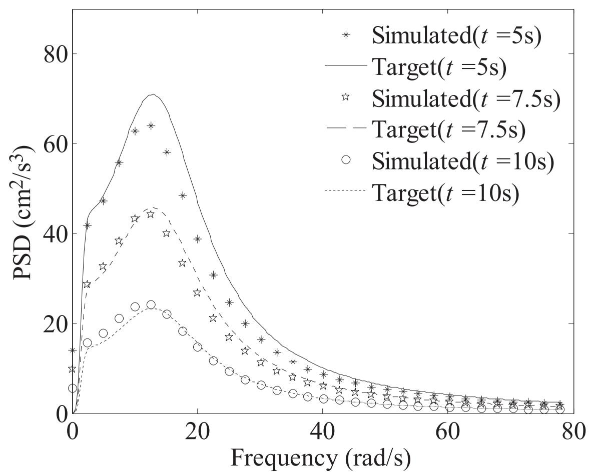

Fig. 9. Target power spectral density and power spectral density of simulated non-stationary seismic acceleration processes by the updated scheme with the non-Gaussian Hartley orthogonal basis at instants of time utilizing the wavelet-based estimation technique in case of sample number $n_{sel} = 626$.

spectral density and power spectral density of simulated non-stationary seismic acceleration processes by the updated scheme with the non-Gaussian Hartley orthogonal basis at instants of time 5 s, 7.5 s and 10 s, utilizing the wavelet-based estimation technique [28]. It is seen that the simulated power spectral density matches well with the target power spectral density, especially in the segments of amplitude attenuation after the instant of time 10 s. In fact, using other random functions such as the Legendre polynomials and the Gaussian Hartley orthogonal basis could gain a desirable simulation results as well. The scaled histograms and probability density functions, moreover, of simulated non-stationary seismic acceleration processes at typical instant of time 10 s using the updated Karhunen-Loeve expansion are pictured in Fig. 10. It is seen that there is a similar result to the stationary case that all the probability density functions are consistent and approach a Gaussian distribution owing to the central limit theorem. The updated scheme has benefit over the conventional through a dimension-reduction technique.

The accuracy of the random function based Karhunen-Loeve expansion in case of simulation for non-stationary processes with respect to the number of representative points is indicated in Fig. 11. It is revealed that similar results to the stationary case, (i) the relative errors are all reduced along with the increment of discretion point number; (ii) the random functions meet with the demand of acceptable error if the sample number $n_{sel} = 626$; (iii) the random functions accommodate a serious zero-mean stochastic process; (iv) among the orthogonal polynomials, the Legendre polynomials and the 1st Chebyshev polynomials are preferentially recommended to be used. All the three types of trigonometric functions could be employed.

Similarly, the non-stationary stochastic process is also represented by the conventional Karhunen-Loeve expansion using

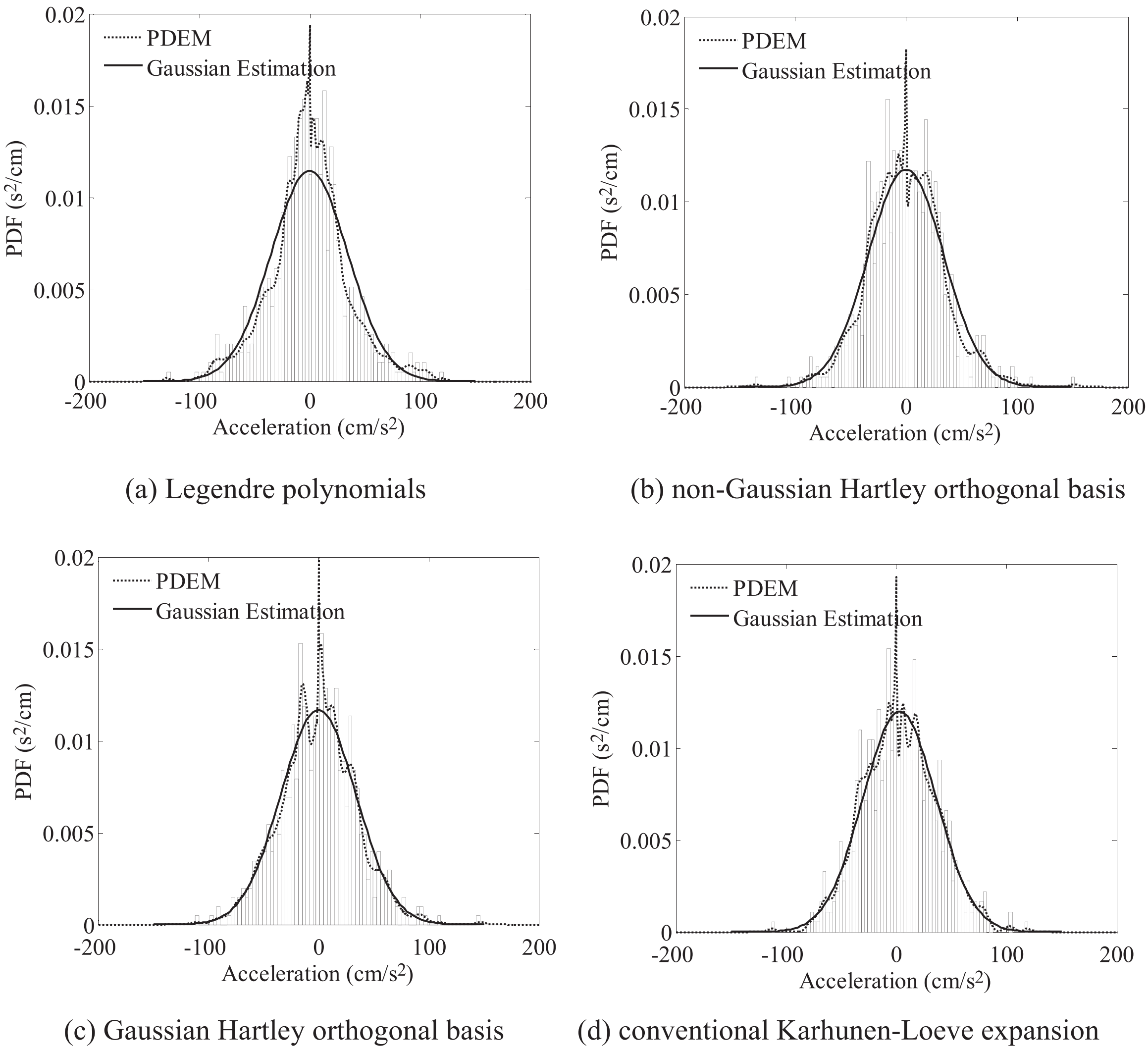

Fig. 10. Scaled histograms and probability density functions of simulated non-stationary seismic acceleration processes at typical instant of time 10 s using the updated and conventional schemes: (a) Legendre polynomials; (b) non-Gaussian Hartley orthogonal basis; (c) Gaussian Hartley orthogonal basis; and (d) conventional Karhunen-Loeve expansion.

the MCS as the generator of samples. It is shown in Table 4 that the average relative errors upon mean, standard deviation and power spectral density by the updated scheme are all smaller than those by the conventional scheme, except the error upon the power spectral density using the Legendre polynomial. It is remarked that the updated Karhunen-Loeve expansion, for both the stationary and the non-stationary stochastic processes, operates more efficiently than the conventional Karhunen-Loeve expansion.

6. Probability density evolution of base-excited nonlinear structures

In recent years, the PDEM has proved its values in the fields of stochastic dynamics of structures, engineering reliability and structural stochastic optimal control [29–31]. Since the discrete representation of seismic ground motion merely relies upon one elementary random variable, the propagation of randomness from the seismic input to the response of structural systems could be efficiently secured through integrating the PDEM with the random function based Karhunen-Loeve expansion. In this section, the response analysis of a nonlinear structure subjected to random seismic ground motions are addressed for illustrative purposes.

Without loss of generality, the equation of motion of an n-degree-of-freedom system is considered as follows

$$\mathbf{M}\ddot{\mathbf{X}}(t) + \mathbf{f}(\mathbf{X}, \dot{\mathbf{X}}, \ t) = \mathbf{\Gamma}\widetilde{X}_g(\mathbf{\Theta}, t) \tag{43}$$

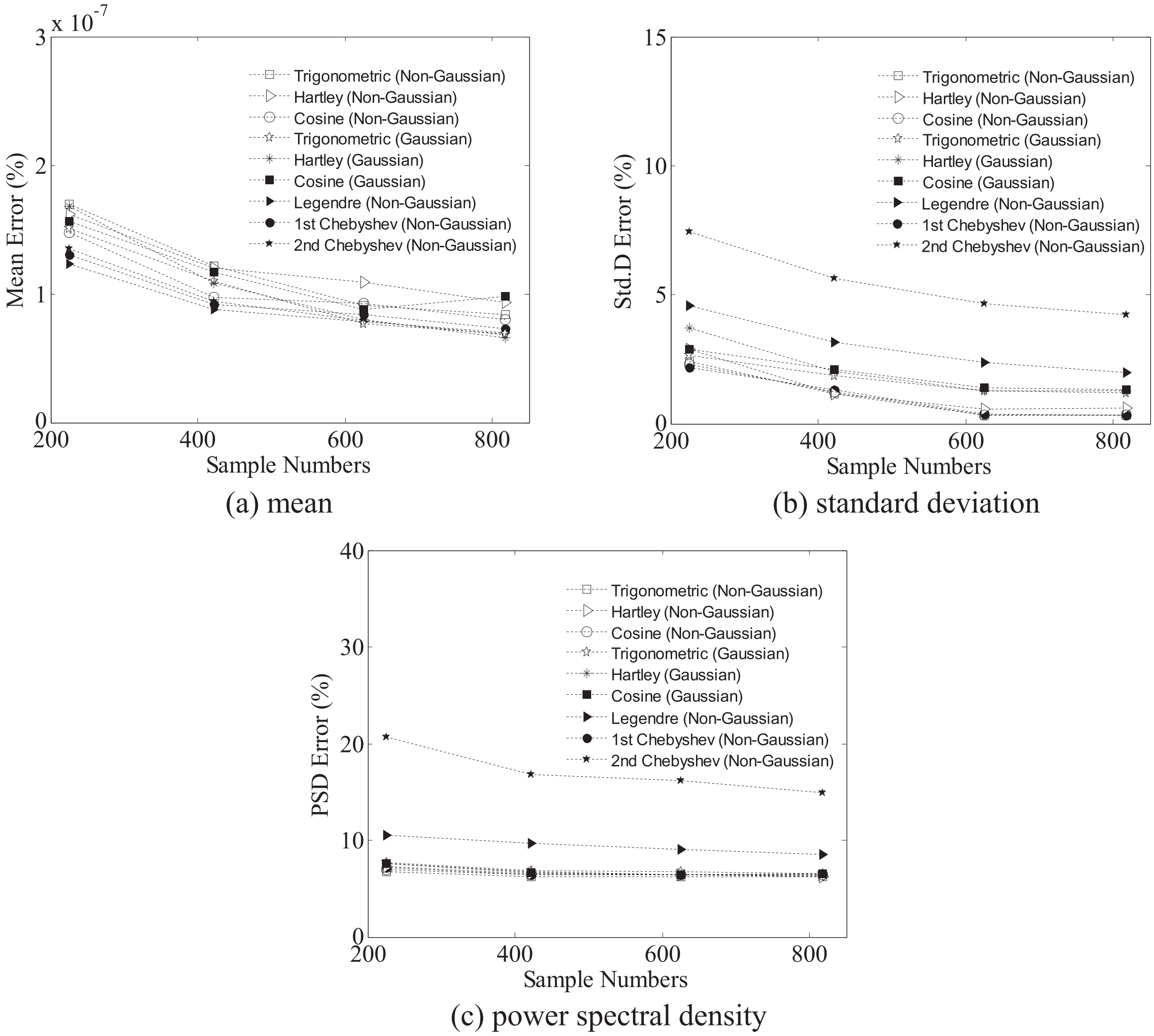

Fig. 11. Average relative errors of the simulated non-stationary processes upon: (a) mean; (b) standard deviation; and (c) power spectral density at instant of time 7.5 s using random function based scheme with different sample numbers.

where the vector $\mathbf{\Theta}$ denotes the randomness inherent in the non-stationary seismic accelerogram $\tilde{X}_g(\mathbf{\Theta}, t)$; the mass vector $\mathbf{\Gamma} = -\mathbf{MI}$, and $\mathbf{I}$ denotes column vector with element 1; $\ddot{\mathbf{X}}, \dot{\mathbf{X}}, \mathbf{X}$ denote the acceleration, velocity and displacement of structure relative to ground motion, respectively; $\mathbf{M}$ denotes the mass matrix of the structure; $\mathbf{f}(\cdot)$ denotes the nonlinear internal-force vector of structure, including damping and stiffness components.

As regards the physical quantities of interest $\mathbf{Z}$, e.g., the displacement, velocity, stress or internal forces, the augmented system $(\mathbf{Z}, \mathbf{\Theta})$ is probability preserved, and is governed by the following generalized probability density evolution equation (GPDEE) [29]

$$\frac{\partial p_{\mathbf{Z\Theta}}(\mathbf{z}, \boldsymbol{\theta}, t)}{\partial t} + \sum_{j=1}^{m} \dot{Z}_j(\boldsymbol{\theta}, t)\frac{\partial p_{\mathbf{Z\Theta}}(\mathbf{z}, \boldsymbol{\theta}, t)}{\partial z_j} = 0 \tag{44}$$

Specifically, as $m = 1$ Eq. (44) becomes

$$\frac{\partial p_{Z\mathbf{\Theta}}(z, \boldsymbol{\theta}, t)}{\partial t} + \dot{Z}(\boldsymbol{\theta}, t)\frac{\partial p_{Z\mathbf{\Theta}}(z, \boldsymbol{\theta}, t)}{\partial z} = 0 \tag{45}$$

The GPDEE is a first-order linear partial differential equation with deterministic initial conditions. The relevant numerical solving procedure refers to the Ref. [29].

Subjected to the seismic ground motion, the components of engineering structures usually expose dynamic behavior with strong nonlinearities. The logical treatment upon the dynamic behavior is building it into a hysteretic model such as bi-

Table 5
Structural parameters of ten-storey shear frame.

Storey	0–1	1–2	2–3	3–4	4–5	5–6	6–7	7–8	8–9	9–10
Mass (1×10^4 kg)	2.4	2.4	2.0	2.0	1.8	1.8	1.6	1.6	1.2	1.2
Pre-yielding Stiffness (kN/mm)	18	18	14	14	12	12	10	10	9.6	9.6
Δ_y (mm)	10.0	10.0	8.0	8.0	8.0	8.0	8.0	8.0	6.0	6.0

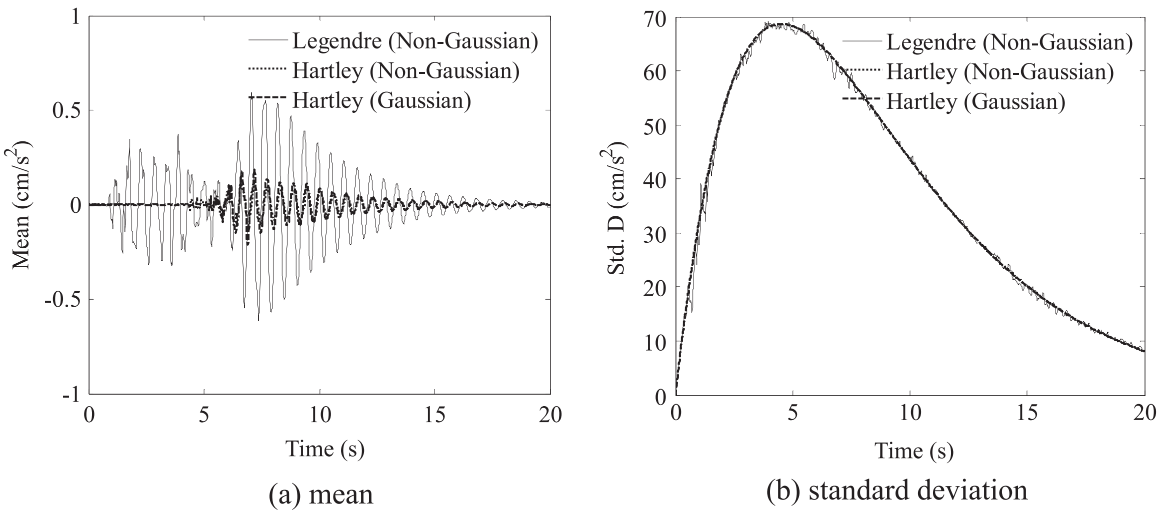

Fig. 12. Statistics of first storey acceleration of structure as to: (a) mean, and (b) standard deviation.

linear functions. A ten-storey shear-framed structure with Clough bi-linear hysteresis is investigated. The storey mass and storey stiffness are shown in Table 5. Rayleigh's damping $\mathbf{C}_t = a\mathbf{M} + b\mathbf{K}_t$, where $\mathbf{K}_t$ denotes the instantaneous stiffness; $a = 0.01$, $b = 0.005$ is employed corresponding to a damping ratio of 1.01% associated with the first vibrational mode. The natural frequencies of the unyielded building are respectively 3.46, 10.00, 15.83, 21.26, 26.57, 31.39, 35.25, 38.64, 41.33, and 44.44 rad/s. Stiffness ratio between yielded component and unyielded component is $\alpha = 0.1$. The initial yielding displacements Δ_y of stories are listed in Table 5, whereby the instantaneous stiffness $\mathbf{K}_t$ can be readily evaluated. The nonlinear dynamic analysis of the bi-linear hysteretic structural system, involved in solving the generalized probability density evolution equations, resorts to the Newmark-β scheme of time integration [23,32].

Since there exists a larger statistical error associated with non-stationary seismic acceleration; see Tables 3 and 4, the random responses of structural system subjected to non-stationary ground motions are investigated. The generated representative samples with number $n_{\text{sel}} = 626$ employing the three random functions, Legendre polynomials, non-Gaussian Hartley orthogonal basis and Gaussian Hartley orthogonal basis, are used in this case as well.

Fig. 12 shows the mean process and standard deviation process of the first storey acceleration. It is seen that the acceleration fluctuation exposes to be more serious where the mean process is not nearly zero process more; see Figs. 8 (a) and 12(a). The random seismic input derived by Legendre polynomials results in a difference from those derived by non-Gaussian Hartley orthogonal basis and Gaussian Hartley orthogonal basis. The structural acceleration responses relevant to non-Gaussian Hartley orthogonal basis and Gaussian Hartley orthogonal basis have a good consistency, as shown in Fig. 12(a) . Besides, the influence of the nonlinear structural system upon the standard deviation of seismic acceleration processes is not so serious that the standard deviation of structural acceleration merely suffers a little change from the that of seismic acceleration processes; see Figs. 8(b) and 12(b).

Fig. 13 shows the probability density functions of the first storey acceleration of structure at typical instants of time 5 s, 10 s and 15 s. It is well revealed that the updated Karhunen-Loeve expansion with the three random functions gains consistent results. One might also realize that the structural response, in the strong non-stationary segment around time instant 5 s, subjected to random seismic input derived by Legendre polynomials exists a variation from those derived by non-Gaussian Hartley orthogonal basis and Gaussian Hartley orthogonal basis. Consistent with the standard deviation of structural response, the distribution of probability density functions becomes narrower with the time propagation from the second after the peak of non-stationary amplitude. The probability density functions at any typical time instants all approach to a Gaussian distribution, indicating that the Gaussian behaviors of seismic ground motions are nearly held during the propagation through the nonlinear structural system. While the peak of probability

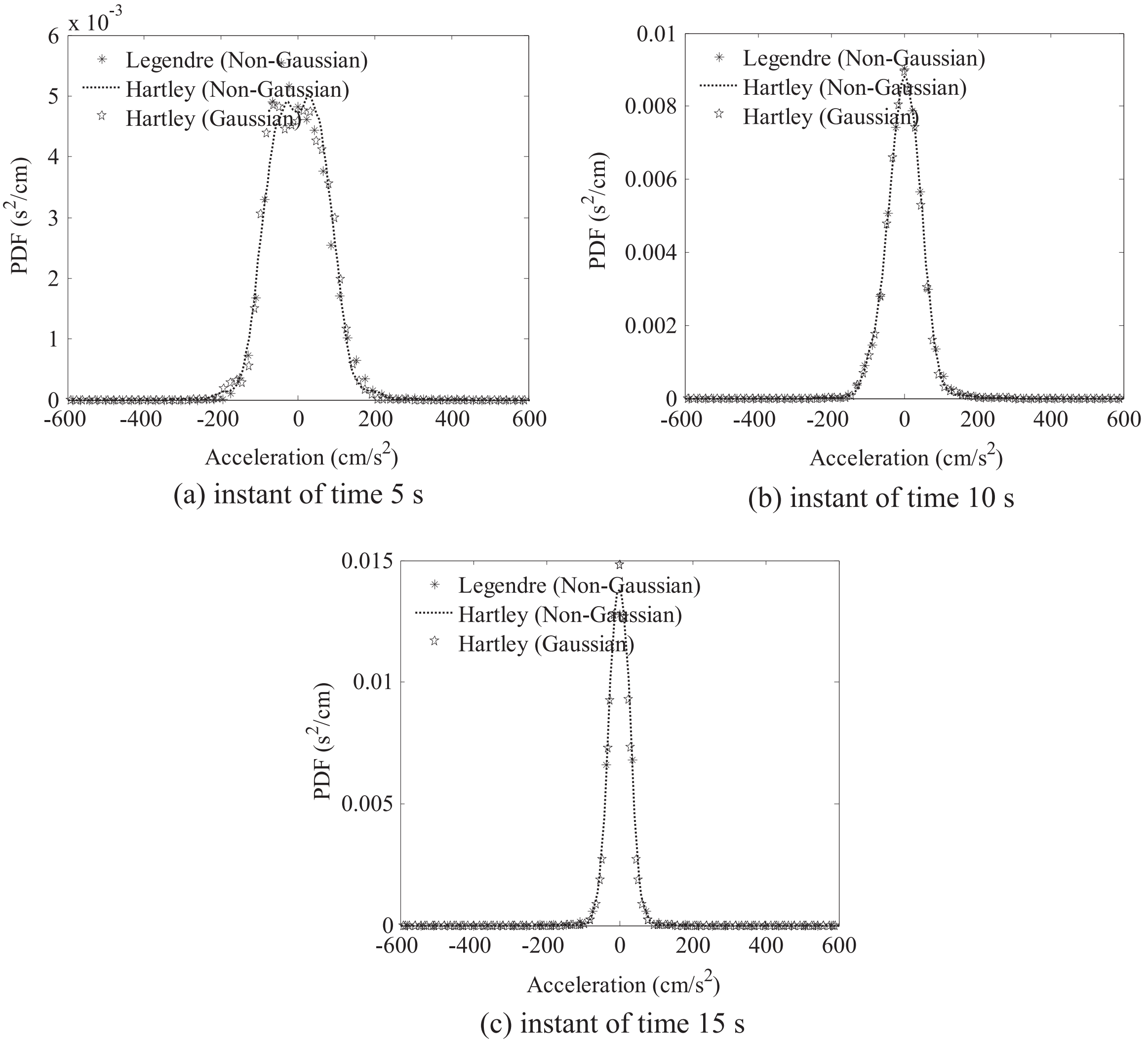

Fig. 13. Probability density function of first storey acceleration of structure at typical instants of time: (a) 5 s; (b) 10 s; and (c) 15 s.

density functions becomes 25% lower; say the probability density function of seismic ground motion and that of structural acceleration at instant of time 10 s; say Fig. 13(b) and Fig. 10, revealing that the nonlinear structural system acts as a filter which enlarges the stochastic fluctuation of seismic ground motion, of which the variability inherent in structural acceleration increases 25%.

7. Conclusions

By introducing random functions as a conditional constraint, the dimension reduction of Karhunen-Loeve expansion is implemented. In the scheme, the random function is expressed as an orthogonal function with a single elementary random variable in polynomial format and trigonometric format. Simulation of seismic acceleration processes and randomness propagation through nonlinear structures reveal the applicability and efficiency of the scheme. Some concluding remarks are summarized as follows:

(1) The random function embedded Karhunen-Loeve expansion with a single elementary random variable bypasses the challenge inherent in the conventional Karhunen-Loeve expansion with hundreds of random variables. The randomness degree of stochastic processes can be effectively reduced from N to 1 by applying the conditional constraint of random functions.
(2) Random functions in the scheme could be expressed as polynomial format (non-Gaussian variables) or trigonometric

format (non-Gaussian and Gaussian variables). The Karhunen-Loeve expansion with orthogonal functions could gain desirable simulation results in case of a moderate sample number, except the Hermite polynomials and the Laguerre polynomials.

(3) The simulated stochastic processes are Gaussian process or approximately Gaussian process, no matter the probability distribution of the random variable subjects to. The simulation accuracy against target statistics can be guaranteed by an appropriate number of expansion terms and representative samples.

(4) The random function embedded Karhunen-Loeve expansion has the benefit of integrating with PDEM, readily for the stochastic analysis of nonlinear structures.

Acknowledgements

The supports of the National Key R&D Program of China (Grant No. 2017YFC0803300), the National Natural Science Foundation of China (Grant Nos. 51278282, 51678450), and the Ministry of Science and Technology of China (Grant No. SLDRCE14-B-20) are highly appreciated. Profs. Jie Li and Jianbing Chen are greatly appreciated for their constructive discussions and comments on the research. The authors are grateful to Mr. Zenghui Liu for his help in preparing the present paper.

References

[1] N.W. Polhemus, A.S. Cakmak, Simulation of earthquake ground motions using autoregressive moving average (ARMA) models, Earthq. Eng. Struct. Dyn. 9 (4) (1981) 343–354.
[2] M. Shinozuka, G. Deodatis, Simulation of stochastic processes by spectral representation, Appl. Mech. Rev. 44 (4) (1991) 191–204.
[3] F. Tubino, L. Carassale, G. Solari, Seismic response of multi-supported structures by proper orthogonal decomposition, Earthq. Eng. Struct.l Dyn. 32 (2003) 1639–1654.
[4] S.P. Huang, S.T. Quek, K.K. Phoon, Convergence study of the truncated Karhunen-Loeve expansion for simulation of stochastic processes, Int. J. Numer. Methods Eng. 52 (9) (2001) 1029–1043.
[5] Z.J. Liu, W. Liu, Y.B. Peng, Random function based spectral representation of stationary and non-stationary stochastic processes, Probab. Eng. Mech. 45 (2016) 115–126.
[6] J.B. Chen, J. Li, Optimal determination of frequencies in the spectral representation of stochastic processes, Comput. Mech. 51 (5) (2013) 791–806.
[7] J.B. Chen, W.L. Sun, J. Li, et al., Stochastic harmonic function representation of stochastic processes, J. Appl. Mech. Trans. ASME 80 (1) (2013) 011001.
[8] J.B. Chen, F. Kong, Y.B. Peng, A stochastic harmonic function representation for non-stationary stochastic processes, Mech. Syst. Signal Process. 96 (2017) 31–44.
[9] D. Wang, J. Li, Physical random function model of ground motions for engineering purposes, Sci. China Technol. Sci. 54 (1) (2011) 175–182.
[10] Z.J. Liu, Y. Wan, B. Zhen, Simulation of stationary ground motion processes: hybrid orthogonal expansion-random function approach, J. Basic Sci. Eng. 22 (2) (2014) 199–208. (In Chinese).
[11] M. Grigoriu, Evaluation of Karhunen-Loeve, spectral, and sampling representations for stochastic processes, J. Eng. Mech. 132 (2006) 179–189.
[12] Y.B. Peng, R. Ghanem, J. Li, Polynomial chaos expansions for optimal control of nonlinear random oscillators, J. Sound Vib. 329 (18) (2010) 3660–3678.
[13] D.B. Xiu, G.E. Karniadakis, The Wiener-Askey polynomial chaos for stochastic differential equations, SIAM J. Sci. Comput. 24 (2) (2002) 619–644.
[14] A.J. Wathen, S.X. Zhu, On spectral distribution of kernel matrices related to radial basis functions, Numer. Algorithms 70 (4) (2015) 709–726.
[15] K.K. Phoon, H.W. Huang, S.T. Quek, Comparison between Karhunen-Loeve and wavelet expansions for simulation of Gaussian processes, Comput. Struct. 82 (2004) 985–991.
[16] F. Kong, J. Li, Wavelet-expansion-based stochastic response of chain-like MDOF structures, J. Sound Vib. 359 (2015) 136–153.
[17] J. Zhang, B. Ellingwood, Orthogonal series expansions of random fields in reliability analysis, J. Eng. Mech. 120 (12) (1994) 2660–2677.
[18] J. Li, Z.J. Liu, J.B. Chen, Orthogonal expansion of ground motion and PDEM-based seismic response analysis of nonlinear structures, Earthq. Eng. Eng. Vib. 8 (3) (2009) 313–328.
[19] M. Loeve, Probability Theory, Springer-Verlag, Berlin, 1977.
[20] R.G. Ghanem, P.D. Spanos, Stochastic Finite Elements: A Spectral Approach, Springer-Verlag, New York, 1991.
[21] Z.K. Liu, Orthogonal Functions and its Applications, National Defence Industry Press, Beijing, 1982 (In Chinese).
[22] J. Li, Stochastic Structural System—Analysis and Modelling, Science Press, Beijing, 1996 (In Chinese).
[23] R.W. Clough, J. Penzien, Dynamics of Structures, 2nd ed. (Revised), Computers and Structures, Inc., Berkeley, 2003.
[24] A. Der Kiureghian, A. Neuenhofer, Response spectrum method for multi-support seismic excitations, Earthq. Eng. Struct. Dyn. 21 (8) (1992) 713–740.
[25] H. Seya, M.E. Talbott, H.H.M. Hwang, Probabilistic seismic analysis of a steel frame structure, Probab. Eng. Mech. 8 (1993) 127–136.
[26] G. Deodatis, Non-stationary stochastic vector processes: seismic ground motion applications, Probab. Eng. Mech. 11 (1996) 149–168.
[27] J.P. Ou, G.Y. Wang, Random Vibration of Structures, Higher Education Press, Beijing, 1998 (In Chinese).
[28] F. Kong, S.J. Li, W.B. Zhou, Wavelet-Galerkin approach for power spectrum determination of nonlinear oscillators, Mech. Syst. Signal Process. 48 (2014) 300–324.
[29] J. Li, J.B. Chen, Stochastic Dynamics of Structures, John Wiley & Sons, Singapore, 2009.
[30] J. Li, J.B. Chen, W.L. Fan, The equivalent extreme-value event and evaluation of the structural system reliability, Struct. Saf. 29 (2) (2007) 112–131.
[31] J. Li, Y.B. Peng, J.B. Chen, A physical approach to structural stochastic optimal controls, Probab. Eng. Mech. 25 (1) (2010) 127–141.
[32] J. Li, Y.B. Peng, J.B. Chen, Nonlinear stochastic optimal control strategy of hysteretic structures, Struct. Eng. Mech. 38 (1) (2011) 39–63.